Report No. IITRI-C6027-16
(Interim Technical Progress Report)

STABLE WHITE COATINGS

July 3, 1964, to March 2, 1965

Contract No. 950746
(Subcontract under NASA Contract NAS7-100)
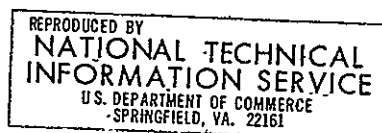IITRI Project C6027

Prepared by

Gene A. Zerlaut, J. E. Gilligan, and Y. Harada

of

IIT RESEARCH INSTITUTE
Technology Center
Chicago, Illinois 60616

for

Jet Propulsion Laboratory
California Institute of Technology
4800 Oak Grove Drive
Pasadena, California

Copy No. _____   June 30, 1965
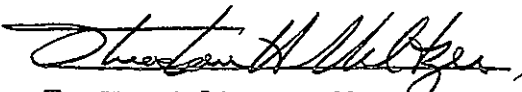
IIT RESEARCH INSTITUTE

FOREWORD

This is Report No. IITRI-C6027-16 (Interim Technical Progress Report) of IITRI Project C6027, Contract No. 950746 (subcontract with the Jet Propulsion Laboratory of the California Institute of Technology under NASA Contract NAS7-100), entitled "Stable White Coatings." The report covers the period from July 3, 1964, to March 2, 1965. This report is prepared for Mr. William F. Carroll, JPL Cognizant Engineer.

Major contributors to the program during this period were Gene A. Zerlaut (Project Leader), John E. Gilligan (zinc oxide photolysis and general consultation), Y. Harada (inorganic coatings), John H. Baldrige (methyl silicone synthesis), Warren E. Jamison and William J. Courtney (space-chamber operation), and Douglas G. Vance and Noel D. Bennett (silicone paint preparations and reflectance measurements). The AH-6 lamp calibration was performed by William J. Courtney. The program was administered by Dr. Theodore H. Meltzer, Manager, Polymer Chemistry.

Data are recorded in Logbooks C14333, C14418, C14475, C14461, C14803, and C14977.

Respectfully submitted,
IIT RESEARCH INSTITUTE

Approved by:

T. H. Meltzer, Manager
Polymer Research

Gene A. Zerlaut
Group Leader
Polymer Research

GAZ/jb/am

IIT RESEARCH INSTITUTE

ii

IITRI-C6027-16

Report No. IITRI-C6027-16
:nterim Technical Progress Report)

STABLE WHITE COATINGS

Jet Propulsion Laboratory

IIT RESEARCH INSTITUTE

ABSTRACT

STABLE WHITE COATINGS

In a previous research program for the Jet Propulsion Laboratory, extensive studies led to the development and specifications of three zinc oxide-pigmented thermal-control coatings. The principal objectives of this program are: improvement of the three paints (as engineering materials), determination of the validity of our accelerated space-simulation testing, and continuation of the zinc oxide photolysis studies begun in the preceding program.

Specific tasks that are discussed include: improvement of potassium silicate coatings as engineering materials and elucidation of their storage and handling problems; improvement of methyl silicone coatings as engineering materials; studies of zinc oxide photolysis to establish reasons for the observed stability of zinc oxide; and determination of space-simulation parameters such as long-term stability (to 8000 ESH), effect of coating surface temperature on the rate of degradation, and validity of accelerated testing (by reciprocity and wavelength dependency studies).

IIT RESEARCH INSTITUTE

IITRI-C6027-16

GLOSSARY

α Solar absorptance.

α_1 and α_2 $\alpha_1 + \alpha_2 = \alpha$.

α_1 corresponds to that half of the sun's energy below 7000 A, and α_2 corresponds to that half above 7000 A.

$\Delta\alpha$ Change in absorptance.

ESH   Equivalent sun-hours of extraterrestrial ultraviolet radiation ($\lambda < 4000$ A).

Me/Si   Molar ratio of methyl groups to silicon atoms.

PVC   Pigment volume concentration.

PBR   Pigment/binder ratio.

TABLE OF CONTENTS

IIT RESEARCH INSTITUTE

IITRI-C6027-16

TABLE OF CONTENTS (cont.)

IIT RESEARCH INSTITUTE

LIST OF TABLES

IIT RESEARCH INSTITUTE

IIT RESEARCH INSTITUTE

LIST OF FIGURES

IIT RESEARCH INSTITUTE

STABLE WHITE COATINGS

I. INTRODUCTION

In a previous research program for the Jet Propulsion Laboratory (Contract 950111, IITRI Project C207), extensive studies led to the development and specification of three zinc oxide-pigmented thermal-control coatings, designated Z93, S-13, and S-33. The zinc oxide pigment used in all three paints is New Jersey Zinc Company's high-purity SP500. The Z93 composition utilizes calcined SP500 and a 35% potassium silicate solution (PS7, Sylvania Electric) as a binder. The S-13 paint is based on General Electric Company's proprietary RTV-602 linear dimethyl-siloxane polymer. The binder used in S-33 is the experimental, molecularly distilled methyl silicone resin developed at IIT Research Institute. Precise specifications of these three coatings as well as the results of the research that produced them are contained in Report No. IITRI-C207-25.

Z93 and S-13 have been shown to be among the most stable coatings available in terms of resistance (increase in solar absorptance) to ultraviolet irradiation in vacuum (ref. 1,2). On the other hand, S-13 is somewhat less resistant to accelerated ultraviolet irradiation than Z93 and S-33 but possesses characteristics that make it very useful as an engineering material. However, S-13 has recently been shown to be inherently stable; reduction of the amine catalyst concentration resulted in a paint with exceptional stability (ref. 3,4).

IIT RESEARCH INSTITUTE

1

The principal objectives of the current program are: improvement of the three paints (as engineering materials), determination of the validity of our accelerated space-simulation testing, and continuation of the zinc oxide photolysis studies begun in the preceding program. Specifically, the tasks include the following:

(1) Improvement of zinc oxide-potassium silicate coatings (Z93) as an engineering material, elucidation of storage and handling problems, and determination of adherence to various substrates.

(2) Improvement of zinc oxide-methyl silicone coatings (S-13 and S-33) as engineering materials, development of a pilot-scale manufacturing procedure for IITRI's experimental methyl silicone resin (used in S-33), and investigation of curing mechanisms for the experimental methyl silicone resins.

(3) Studies of zinc oxide photolysis to establish reasons for the observed stability of zinc oxide and correlation of the photolysis mechanism with stability to the simulated space environment.

(4) Determination of the following space-simulation parameters: long-term stability (by testing an equivalent of one-year exposure under space conditions), effect of coating (surface) temperature on the rate of degradation, and validity of accelerated testing (by reciprocity and wavelength dependency studies).

In general, the tasks and requirements enumerated above were completed during the program. The studies outlined for S-13 and S-33 (task 2) were modified when (1) it became necessary on other programs (ref. 3,5) to elucidate the field-application potential of S-13 for use on the Pegasus A and B satellites and associated Saturn stages, and (2) the excellent stability and optical properties of Owens-Illinois type 650 glass resin became apparent;

II-T RESEARCH INSTITUTE

2

IITRI-C6027-16

the latter finding lessened the urgency for scaling up the manufacture of the experimental methyl silicone resin used in the S-33 coating. Therefore, studies on S-13 and S-33 coatings were limited during this report period to completion of work begun during the first half of the program and to the preparation and irradiation of S-13 and S-33 specimens in support of task 4 (which included long-term testing and temperature, reciprocity, and wavelength dependency studies).

Although this report covers the period from the Semiannual Report (ref. 6) to the present, information and data contained in the earlier publication were abstracted or otherwise used to implement and complete the discussions and conclusions presented in the ensuing paragraphs. In addition to major sections on zinc oxide-pigmented silicate and silicone paints, zinc oxide photolysis and simulation parameters, sections in which we discuss such problem areas as lattice distortion, contamination, specimen handling, and accelerated testing are also presented. Ancillary experiments designed to obtain a UV-band-pass filter and to determine the AH-6 lamp output (solar factor) versus distance are contained in Appendices I and II. Up-to-date specifications of S-13 and Z93 are presented in Appendix IV.

II. SPACE SIMULATION

A. Reflectance Measurements and Calculations of Solar Absorptance

Solar absorptance is determined indirectly by measurement of spectral reflectance in the wavelength range 0.325 to 2.7 μ (325 to 2700 mμ). The reflectance data are integrated with extra-terrestrial solar spectral energy data to yield solar absorptance by using a Fortran II program developed for the IBM 7094 computer. Solar absorptance is split into two components, α_1 and α_2, so that the region of the spectrum undergoing the most significant change in absorptance (i.e., many specimens bleach in the near infrared) can be more readily described. A comprehensive discussion of this program is presented in Appendix I of the Semi-annual Report.

Spectral reflectance was measured with a Cary model 14 spectrophotometer equipped with the model 1411 integrating-sphere accessory in all tests (listed in Table 1) except Q-8 through Q-11. Reflectance values associated with Quad-Ion tests Q-8 through Q-11 were measured with the Beckman DK-2A spectroreflect-ometer.

The Cary 14 is described in the Semiannual Report. It is comparison type of integrating-sphere reflectometer, which is used with Type II illumination, in which the illuminating beam falls on the sphere wall, and the sample and the reference subsequently receive nondispersed, diffuse illumination. The reflectance is measured as the ratio of the brightnesses when

IIT RESEARCH INSTITUTE

4

IITRI-C6027-16

the detector optics alternately view the sample and reference specimens.

The Beckman DK-2A is a ratio-recording spectrophotometer and, unlike the Cary 14, utilizes monochromatic incident light. It uses Type I operation, in which the specimen reflectance is determined as the ratio of sphere wall brightnesses when first the specimen and then the reference standard are illuminated. The advantages of the Beckman DK-2A are, excluding accuracy considerations, (1) its greater wavelength span and (2) the elimination of the possibility of sample bleaching during measurement as a result of using monochromatic rather than nondispersed light.

The question of a comparative accuracy between the two instruments arose when it was noted that the solar absorptances computed from DK-2A data generally were 0.02 to 0.03 lower than those computed from Cary 14 data. This was subsequently traced to the fact that the Vitrolite secondary standard employed in both cases showed from 4 to 5% higher reflectance when measured on the Beckman instrument. The two instruments agreed to within 1% when S-13 and Z93 were compared to the same magnesium oxide/magnesium carbonate standard.

The difference in reflectance of the Vitrolite when measured on the two instruments is attributed to the fact that it is translucent and semitransparent. Therefore, since a thick specimen is required to obtain moderately high reflectance, the illumination and viewing conditions are quite different, and the conditions required for reciprocity are, in reality, not

achieved. Since the main requirement for the secondary standard is that it must not undergo reflectance changes over a considerable period of time, an opaque surface such as a highly reflecting porcelain enamel should be more suitable as a standard.

Although the two instruments agree to within 1% when white coatings are measured, the Beckman DK-2A is generally higher for surfaces that exhibit some gloss. An anomaly, however, is the fact that polished aluminum exhibits an approximately 5% higher reflectance when measured with the Cary 14. This same relation was noted in studies on an integrating-sphere reflectometer capable of making both Type I and Type II measurements (ref. 7) (This is accomplished by rotating the sphere exactly 180°, thus reversing the functionality of the entrance and exit ports). In this case, it was concluded that the light incident upon the sample in Type II illumination was not completely diffuse.

B. Simulation Chambers and Equipment

Test V-54 through V-63 utilized the 400-liters/sec VacIon ion-pumped chamber described in Report No. IITRI-C207-25. Tests Q-6 through Q-12 utilized the Quad-Ion space-simulation facility described in Figures 1 through 3 of the Semiannual Report. The four chambers in the Quad-Ion facility are pumped with 140-liters/ sec Ultek ion pumps. The chambers in both facilities are equipped with liquid-cooled specimen tables; in these tests the samples were epoxied to the metal tables. They were heated with hot water during evacuation and final pumpdown and were maintained at cold tap-water temperature ($\sim$10°C) during irradiation.

IIT RESEARCH INSTITUTE

6

Specimens irradiated in tests D-1 through D-2 were evacuated
chamber that was constructed for the oil-diffusion pumping
station (4000 cfm, NRC model H-10-SP) described in Report No.
IITRI-C207-25. The cylindrical chamber is 24 in. in diameter and
employs a flat head with a quartz window mounted in the center.
The AH-6 lamp is mounted externally to the chamber; the samples,
which are discussed in Section V-A, are mounted to a resistance-
heater element for use in the high-temperature tests.

C. Space-Simulation Parameters

Pertinent data are presented in Table 1. The nominal sample
temperature was determined with a shielded thermocouple peened
into the temperature-controlled sample table both in the 400-
liters/sec VacIon system and in the Quad-Ion system.

The solar intensity-exposure values for test Q-8 were
calculated from a day-to-day plot of solar intensity versus time.
The bar graph from which the Q-8 data were computed is presented
in Appendix I and is representative of the plots made for the
various tests reported.

The AH-6 lamp calibration is discussed in Appendix II.
Although all data in this report are based on the "old" calibra-
tion, i.e., 50% of the AH-6 lamp's energy is assumed to be below
4000 A, the exposure and solar intensity data should be multiplied
by 0.76 to be more accurate. The "new" calibration assumes that
38% of the lamp's energy is below 4000 A. The old calibration
was used in this report in order to make the sun-hour exposure
data consistent with previously reported data.

<div align="center">IIT RESEARCH INSTITUTE</div>

7

Table 1

PERTINENT DATA ON SPACE-SIMULATION TESTS

Test No.	Average Solar Factor	Time, hr	Exposure, ESH	Operating Pressure, torrs		Sample Temp.,
				Initial	Terminal	
V-39[a]	10.5	200	2100	1.5×10^{-5}	3.0×10^{-8}	+43
V-49	8.0	265	2120	3.0×10^{-6}	1.2×10^{-8}	+43
V-51	10.0	200	2000	5.0×10^{-6}	8.5×10^{-9}	+50
V-52	11.7	85	1000		$<3.0 \times 10^{-5}$	>+50
V-54	8.9	228	2030		$<3.0 \times 10^{-5}$	+45
V-56	10.1	207	2100	7.0×10^{-6}	9.5×10^{-9}	+43
V-57	9.2	77	710	5.0×10^{-5}	8.0×10^{-8}	b
V-60	10.0	216	2160	1.0×10^{-6}	1.0×10^{-7}	+43
D-1	4.5	89	400		$<1.0 \times 10^{-5}$	+425
D-2	5.5	73	400		$<1.0 \times 10^{-5}$	+610
D-3	5.0	88	440	4.1×10^{-6}	1.5×10^{-6}	+500
Q-6 Aborted						
Q-7-1	4.1	207	850	2.0×10^{-7}	1.2×10^{-8}	+43
Q-7-II[c]	4.1	207	850	5.0×10^{-6}	1.8×10^{-7}	+43
Q-7-III	4.1	207	850	5.0×10^{-6}	1.8×10^{-7}	+43
Q-7-IV[c]	4.1	194	810	3.0×10^{-7}	2.2×10^{-8}	+43
Q-8-I	3.9	260	1010	6.0×10^{-7}	7.0×10^{-8}	+41
Q-8-II	14.4	87	1250	3.0×10^{-6}	3.0×10^{-6}	+41
Q-8-III	3.9	260	1010	9.0×10^{-7}	2.5×10^{-8}	+41
Q-8-IV	14.4	87	1250	3.0×10^{-6}	3.0×10^{-6}	+41
Q-9-I	5.0	221	1110	2.0×10^{-6}	2.2×10^{-6}	+43
Q-9-II	5.0	221	1110	4.0×10^{-6}	2.2×10^{-8}	+43
Q-9-III	5.0	221	1110	7.0×10^{-7}	6.0×10^{-8}	+43
Q-9-IV	5.0	221	1110	7.0×10^{-7}	7.0×10^{-8}	+43
Q-10-I	5.8	361	7900	3.5×10^{-8}	$<3.0 \times 10^{-8}$	+43
Q-10-III	5.8	361	7900	3.5×10^{-6}	$<3.0 \times 10^{-8}$	+43
Q-11-II	4.8	56	300	1.8×10^{-6}	$<1.0 \times 10^{-6}$	+43
Q-11 IV	4.8	56	300	3.2×10^{-6}	$<1.0 \times 10^{-6}$	+43
Q-12-II	6.1	738	4500	5.0×10^{-6}	1.6×10^{-6}	+43
Q-12 IV	6.1	738	4500	2.0×10^{-6}	2.7×10^{-7}	+43

[a] V-39 included fro   ITRI-C6027-7 for comparison.

[b] Powder compacts.

[c] Filtered with Corning 7-54.

III. ZINC OXIDE-POTASSIUM SILICATE PAINTS

The final phase of this program was concerned with optimizing the optical and physical properties of Z93. The following evaluations were included in these studies.

(1) Effect of time on reflectance

(2) Effect of curing variables on stability

(3) Effect of storage media on stability

(4) Effect of curing conditions on physical properties

Coating designations previously used are correlated with current designations in Appendix III. An up-to-date specification for Z93 is given in Appendix IV.

A. Optical Properties

The effect of time on the reflectance of heat-treated Z93 and silicate-bonded zirconia was examined. The solar absorptance changes for the two samples are given in Table 2.

Table 2

EFFECT OF HEAT TREATMENT AND TIME
ON REFLECTANCE OF SILICATE-BONDED COATINGS

Sample	Time Lapse	Treatment	Solar Absorptance		
			α_1	α_2	α
6001	0	None	.090	.074	.164
(Z93)	1 day	145°C/16 hr	.090	.069	.158
	6 hr	500°C/2 hr	.085	.064	.149
	3 mo	None	.087	.073	.160
6002	0	None	.069	.106	.175
(ZrO$_2$)	1 day	500°C/2 hr	.075	.091	.166
	3 mo	None	.076	.108	.184

IIT RESEARCH INSTITUTE

9

Reflectance measurements of both samples after a 3-month lapse showed that the infrared reflectance values had returned to those of the original untreated samples. The visible and ultraviolet reflectance were essentially unchanged by heat treatment. These silicate systems are apparently absorbing water on standing, as indicated by the reappearance of a broad absorption band at 1.9 μ.

Higher heat treatments to 800°C were facilitated by using substrates of dense magnesium silicate (2 MgO·SiO$_2$) and alumina. Changes in coating weight as well as solar absorptance were recorded as a function of temperature and time. Results of this experiment are tabulated in Table 3.

Table 3

EFFECT OF ELEVATED TEMPERATURES ON REFLECTANCE OF Z93

Sample	Time Lapse	Treatment	Weight Change, %	Solar Absorptance		
				α_1	α_2	α
6003	0	None	0	.092	.073	.165
(on Mg$_2$SiO$_4$)	1 day	145°C/16 hr	−3.1	.089	.069	.158
	6 day	500°C/2 hr	−1.2	−	−	−
	1 day	700°C/2 hr	−1.1	.092	.066	.158
	6 hr	800°C/2 hr	−0.5	.093	.066	.159
	3 mo	None	+0.4	.094	.067	.161
6004	0	None	0	.094	.074	.168
(on Al$_2$O$_3$)	1 day	145°C/16 hr	−3.0	.091	.068	.159
	6 hr	500°C/2 hr	−1.3	−	−	−
	1 day	700°C/2 hr	−1.1	.094	.066	.160
	6 hr	800°C/2 hr	−0.4	.095	.067	.162
	3 mo	None	+0.3	.097	.068	.165

IIT RESEARCH INSTITUTE

IITRI-C6027-16

The α_2 column shows that the 800°C heat treatment apparently minimized the reabsorption of water. The reflectance curves reveal only a small hint of the 1.9-μ band. The gravimetric analysis also reveals that water pickup was minor.

1. Effect of Sample Treatment

Experiment V-52 was conducted for 1000 ESH to investigate the effects of substrate cooling, heat treatment, and water immersion on the stability of Z93. Sample 6005 was epoxy-cemented onto the water-cooled sample table in the space chamber; the other samples were merely placed on the table and conceivably attained temperatures of 100°F. Sample 6006 was immersed in distilled water for 16 hr and then dried with prepurified nitrogen. Sample 6008 was heated at 300°C for 2 hr; 6007 received no special treatment. Data for these Z93 compositions are presented in Table 4.

Table 4

UV-VACUUM RESISTANCE OF Z93 COATINGS
RECEIVING VARIOUS TREATMENTS (TEST V-52)

| Sample | Treatment | Exposure, ESH | Solar Absorptance | | | |
			α_1	α_2	α	$\Delta\alpha$
6005	None	0	.082	.071	.153	
		1000	.088	.071	.159	.006
6006	Water immersion	0	.083	.064	.147	
		1000	.101	.065	.167	.020
6007	None	0	.086	.079	.165	
		1000	.101	.078	.179	.014
6008		0	.083	.071	.153	
	300°C/2 hr	0	.082	.071	.153	
		1000	.092	.069	.160	.007

11

The better stability of a cooled sample and also of a heat-treated sample is shown by the results for 6005, 6007, and 6008. The poor thermal contact with the sample table probably caused 6007 to be hotter, causing greater degradation. The water-immersed sample sustained the greatest change in reflectance, suggesting that the water content has a detrimental effect.

In space-simulation experiment V-56 the effect of water on the degradation of Z93 coatings was determined. The test was conducted for 2100 ESH. Optical data history as a result of treatments and ultraviolet-vacuum are presented in Table 5.

Samples 7012 and 7013 showed increased infrared reflectance as a result of heat treatment; the control sample, 7011, had virtually the same spectral curve. After one month, all samples showed a decrease in infrared reflectance. The gravimetric analysis indicated water pickup for 7012 but not for 7013. The reappearance of the water absorption peak at 1.9μ was evident for both of these samples, although it was more pronounced for 7012. Very small solar absorptance changes due to the ultraviolet-vacuum occurred. No rigorous distinction could be made relating to the histories of Z93 samples.

Sample 7016 was a Z93 coating that had been wrapped in aluminum and thus received no ultraviolet irradiation. As reflected in the α_2 values and as clearly shown by the spectral curves, a bleaching effect was evidenced in the $1.6-$ to $2.0-\mu$ region. The relatively small $\Delta\alpha$ for the ZrO_2 sample, 7015,

IIT RESEARCH INSTITUTE

12

Table 5

UV-VACUUM RESISTANCE OF Z93 COATINGS
RECEIVING VARIOUS TREATMENTS (TEST V-56)

Sample	Treatment	Weight Change, g	Solar Absorptance			
			α_1	α_2	α	$\Delta\alpha$
7001	None		.084	.069	.153	
	+6 hr	-0.0002	.085	.069	.154	..001
	+1 mo	-0.0001	.086	.074	.159	..005
	2100 ESH		.091	.072	.163	..004
7012	None		.085	.070	.154	
	500°C/2 hr	-0.0043	.085	.063	.148	-.006
	Lab conditions[a]	+0.0030	.088	.073	.160	.012
	2100 ESH		.091	.072	.163	..003
7013	None		.084	.069	.153	
	500°C/2 hr	-0.0040	.085	.060	.145	-.008
	Stored[b]	+0.0001	.086	.069	.155	.010
	2100 ESH		.094	.071	.165	.010
7016	None		.085	.073	.159	
	2100 ESH[c]		.086	.069	.155	-.004
7015[d]	None		.075	.124	.199	
	2100 ESH		.119	.121	.240	.041,

[a]35% Relative humidity, 1 month.

[b]Stored over Drierite desiccant, 1 month.

[c]Sample 7016 was wrapped in aluminum during the test and did not see UV.

[d]Zirconia-silicate sample.

Note: Sample 7011 was remeasured along with samples 7012 and 7013 when their spectral curves were determined after the heat treatment and storage.

suggests that the exposure of the experiment was less than 2000 ESH.

Samples of Z93 cured under 100%, 35%, and 0% relative humidity (RH) were subjected to 2160 ESH in Test V-60. Excellent stability was exhibited by all samples, showing no deleterious effect of either an extremely wet or dry condition during cure. The results, along with α changes for a ZrO_2 sample, appear in Table 6. These experiments (V-52, V-56, V-60) suggest that the presence of small amounts of residual water in Z93 coatings is not harmful to ultraviolet-vacuum resistance.

Table 6

EFFECT OF CURE HUMIDITY
ON UV-VACUUM RESISTANCE OF Z93 (TEST V-60)

| Sample | Relative Humidity during Cure | Exposure, ESH | Solar Absorptance | | | |
			α_1	α_2	α	$\Delta\alpha$
7071	100%	0	.087	.066	.153	
		2160	.092	.067	.159	.006
7072	0%	0	.091	.077	.168	
		2160	.097	.077	.174	.006
7073	35%	0	.089	.072	.161	
		2160	.093	.072	.165	.004
7070	(ZrO_2-silicate)	0	.076	.124	.200	
		2160	.136	.126	.262	.062

Space-simulation experiment V-57 (710 ESH) included two Z93 samples with different histories. Sample 7021 was a Z93 coating from a group prepared about a year ago for evaluation

IIT RESEARCH INSTITUTE

4

by other agencies. The Space Technology Laboratory* had found them to be quite unstable, exhibiting $\Delta\alpha$'s in excess of 0.20 after 500 ESH. This particular sample was returned unirradiated to IITRI by STL for examination. This experiment (V-57) revealed a very small $\Delta\alpha$ for this sample. Although the companion Z93 (7020) showed less degradation, the age of sample 7021 plus excessive handling could have introduced a slight contamination. The results appear in Table 7.

Table 7

EFFECT OF SAMPLE HISTORY
ON UV-VACUUM RESISTANCE OF Z93 (TEST V-57)

Sample	Description	Exposure, ESH	Solar Absorptance			
			α_1	α_2	α	$\Delta\alpha$
7019	ZrO_2-silicate	0	.073	.125	.197	
		710	.128	.121	.249	.052
7020	Z93	0	.082	.070	.152	
		710	.093	.069	.161	.009
7021	Z93 prepared for evaluation by STL	0	.093	.077	.170	
		710	.111	.077	.187	.017

2. Effect of Plastic Storage

Although early experiments indicated that soiled Z93 could be adequately cleaned for retention of stability, a preferable procedure would be prevention of contamination. Thus, an experiment was designed to evaluate the effect of plastic storage on

---

*Bevans, J. T., Private Communication.

IIT RESEARCH INSTITUTE

IITRI-C6027-16

subsequent ultraviolet-vacuum resistance of Z93. Samples were prepared, cured, and stored in plastics in a static air environment, and groups of these were examined after 3-, 8-, and 14-month periods.

The data tabulated in Table 8 show that all the plastics provided excellent protection. Changes in solar absorptance were all very small. All tests included zirconia-silicate coatings as degradable standards; the $\Delta\alpha$ range for this system is usually 0.07 to 0.09 after about 2000 ESH. The data from test V-39 were the only data that varied from this range and suggest a higher ESH.

Another factor that contributed to the desirable behavior of Z93 samples was probably the limited amount of handling they received. They were stored in a closed container, which was opened only for removal of specimens after the test periods. Although the container was by no means gastight, a relatively static environment was maintained.

The solar absorptance values for test 39 are somewhat lower than those for tests 49 and 60 because of a change in measuring techniques. From test 1 through test 39, α was measured with a GE spectrophotometer for the visible range and an IITRI-designed integrating-sphere reflectometer for the ultraviolet and infrared regions. In tests 40 through 60, the Cary 14 with the model 1411 reflectance attachment was used. The α_1 values measured by either instrument are similar. However, the α_2 values measured with the Cary are about 0.01 higher than those

IIT RESEARCH INSTITUTE

16

Table 8

EFFECT OF UV IRRADIATION IN VACUUM ON Z93 COATINGS STORED UNDER PLASTICS

Sample	Storage Medium	Time, mo	Test	Exposure, ESH	Solar Absorptance α_1	α_2	α	$\Delta\alpha$
6009	Mylar	3	39	0	.093	.074	.168	
				2100	.103	.068	.171	.003
6016	Mylar	8	49	0	.097	.086	.183	
				2120	.107	.081	.189	.006
7074	Mylar	14	60	0	.094	.082	.176	
				2160	.099	.077	.176	000
6010	H–polymer	3	39	0	.097	.077	.173	
				2100	.111	.072	.183	.010·
6017	H–polymer	8	49	0	.101	.091	.192	
				2120	.110	.082	.192	.000
7075	H–polymer	14	60 ·	0	.094	.084	.178	
				2160	.098	.076	.175	−.003
6011	Lexan	3	39	0	.098	.077	.175	
				2100	.112	.074	.186	.011
6018	Lexan	8	49	0	.098	.087	.185	
				2120	.108	.087	.194	.009
7076	Lexan	14	60	0	.096	.086	.183	
				2160	.097	.081	.179	−.004
6012	Teflon type A	3	39	0	.098	.082	.180	
				2100	.116	.075	.190	.010
6019	Teflon type A	8	49	0	.096	.085	.181	
				2120	.108	.081	.189	.008
7077	Teflon type A	14	60	0	.097	.085	.182	
				2160	.102	.083	.184	.002
6013	Tedlar	3	39	0	.097	.075	.172	
				2100	.116	.073	.189	.017
6020	Telar	8	49	0	.098	.088	.186	
				2120	.111	.084	.196	.010
7078	Tedlar	14	60	0	.095	.086	.181	
				2160	.098	.081	.180	−.001
6014	Vellum	3	39	0	.100	.084·	.183	
				2100	.117	.073	.190	.007
6021	Vellum	8	49	0	.100	.089	.189	
				2120	.112	.085	.197	.008
7079	Vellum	14	60	0	.097	.087	.184	
				2160	.102	.085	.187	.003
6015[a]	Vellum	2	39	0	.063	.114	.176	
				2100	.186	.118	.303	.127
6022[a]	Vellum	2	49	0	.068	.109	.176	
				2120	.150	.109	.259	.083
7070[a]	Vellum	4	60	0	.076	.124	.200	
				2160	.136	.126	.262	.062

[a]Zirconia–silicate controls.

IITRI–C6027–16

obtained with the GE equipment. This slight variance has been found with samples in other tests as well. Changes in solar absorptance were not affected, however, since all reported values reflect measurements from the same instrument before and after simulation.

B. Physical Properties

1. Effect of Curing Conditions

Experiments were conducted to determine the effects of relative humidity during curing upon the physical properties of Z93 coatings. Three sets of samples were prepared at the same time from one formulation and cured and stored for one month under the following conditions: 100% RH; 35% RH (laboratory bench); and in a desiccator over Drierite, or essentially 0% RH. These samples are numbered 6031 through 6039 and are designated series A for descriptional clarification.

After being removed from the extreme conditions to the laboratory environment, the samples were examined under 10X magnification. Some of the thicker coatings (7 to 8 mils) from the 0% RH showed slight cracking at the edges; coatings of comparable thicknesses stored in the other environment revealed no such flaws. The 100% RH samples were quite soft in comparison with the others as determined by a simple scratch test.

Three 1 x 3-in. specimens from each set were subjected to torsion. Best adhesion was exhibited by the 0% RH coatings and the poorest adhesion by samples cured in 100% RH. Data for

IITRI-C6027-16

these measurements are shown in Table 9, and are graphically represented in Figure 1. Since gravimetric measurements of thickness are more accurate than micrometer measurements, weights are represented on the abscissa. A plot of weight versus thickness reveals a relationship of 0.1 (n) grams $\simeq$ n mils.

A second experiment (series B) was conducted by duplicating the curing conditions described above. The environments and observed physical effects were as follows.

(1)   100% relative humidity -- Sample surfaces were wet upon removal from the "wet" room 48 hr after application. After being dried in air for 24 hr, the surfaces appeared glazed and specular, unlike the air-cured matte-finish coatings. An extremely smooth finish was observed under 10X magnification. These coatings had formed a hard, silicate-rich topcoat , unlike the 100% RH samples of the earlier experiment.

(2)   35% relative humidity -- Samples were cured under ordinary laboratory conditions. No discontinuity was noted under 10X magnification.

(3)   0% relative humidity -- Samples were cured and stored for 5-1/2 days in a desiccator over Drierite. No discontinuity was observed under 10X magnification.

(4)   Air dry and oven cure -- After a 24-hr air dry, this group was placed in an oven at 140°C for 24 hr. Very faint cracks along the edges were discerned under 10X magnification.

(5)   Flowing air -- These samples were subjected to a rapid flow of air in a hood. Cracking along the edges was visible to the eye within 1/2 hr. Examination under 10X magnification revealed the cracking to be confined to the edges only; the central area showed no discontinuity.

(6)   Infrared lamp -- A thermometer check showed the temperature to be 60°C for the samples placed under an infrared lamp. Cracking at the edges and integrity of the central area were very similar to that observed for the "flowing air" samples.

IIT RESEARCH INSTITUTE

19

Table 9

TORSION RESISTANCE OF Z93
AS A FUNCTION OF CURING CONDITIONS

Curing Conditions	Sample	Weight, g	Thickness, mils[a]	Angle at Failure, °
100% RH	6031	0.511	5.5	27
	6032	0.570	5.75	27
	6033	0.496	5.25	26
100% RH	6041	0.735	8.0	14
	6042	0.804	9.0	12
	6043	0.902	10.5	12
35% RH	6034	0.545	5.5	37
	6035	0.543	5.25	36
	6036	0.634	6.0	32
35% RH	6044	0.529	5.5	56
	6045	0.544	5.5	54
	6046	0.673	7.5	53
0% RH	6037	0.642	6.0	57
	6038	0.546	5.5	75
	6039	0.535	5.5	78
0% RH	6047	0.599	6.0	96
	6048	0.590	6.0	97
	6049	0.656	7.5	83
Air dry and oven cure	6050	0.701	7.0	37
	6051	0.627	6.5	40
	6052	0.676	7.5	44
Air flow	6053	0.614	7.0	38
	6054	0.580	6.0	41
	6055	0.721	7.5	25
IR lamp	6056	0.519	5.0	46
	6057	0.524	5.5	47
	6058	0.644	7.0	36

[a]Measured with micrometer.

IITRI-C6027-16

Figure 1

EFFECT OF CURING CONDITIONS ON TORSION RESISTANCE OF Z93 COATINGS
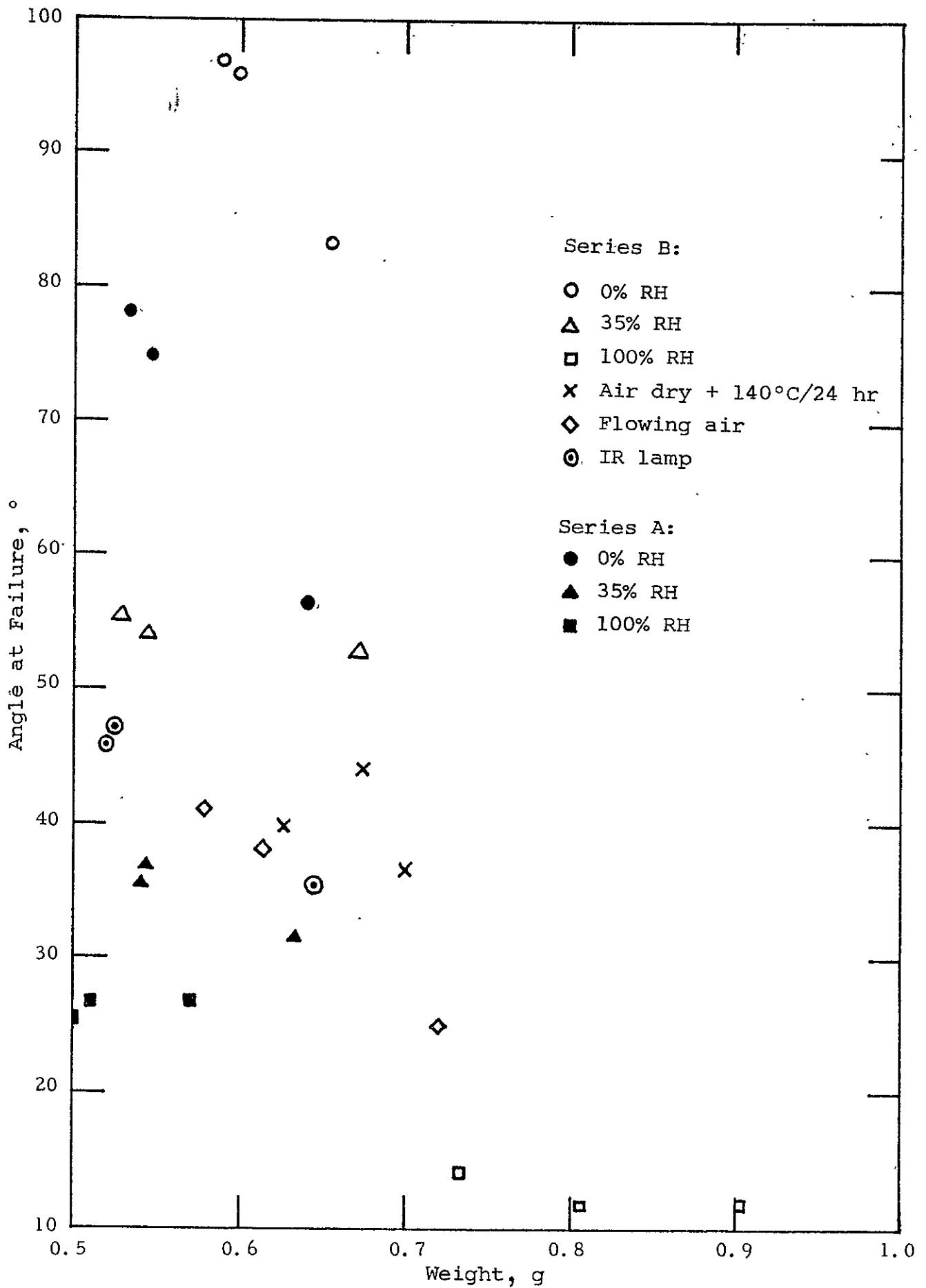
Torsion tests revealed the superior adhesion of samples cured at 0% RH; those cured at 100% RH were clearly inferior. Better adhesion was exhibited by the series B samples in comparison with their series A counterparts, except for the 100% RH samples; the weight differentials obscure any rigid comparison.

Drying was accelerated by exposing samples to a flow of air and also by heating with an infrared lamp. As mentioned above, edge cracks in these coatings resulted. The data show that failure occurred at lower angles than for the specimens cured by normal air drying. Heat curing after a 24-hr air dry also failed to improve the twist resistance. Thus, for best adhesion, the ideal condition is a dry, static atmosphere at room temperature.

IV. ZINC OXIDE-METHYL SILICONE PAINTS

A. S-13 Coatings

One of the program's tasks was to improve the S-13 coating as an engineering material, but this task was terminated when it became necessary to determine rapidly the field-application potential of the S-13 system for use on the Pegasus satellites and their associated Saturn upper stages. These studies, which were performed on other programs (ref. 3,5), resulted in the establishment of the more important manufacturing and application parameters necessary for the utilization of large quantities of the S-13 thermal-control paint. Approximately 135 gal of S-13, manufactured in 5-gal lots, has been furnished to the Engineering Materials Division of NASA's George C. Marshall Space Flight Center for application on location at Cape Kennedy, Florida. The results of these field-application studies are presented in the up-to-date S-13 specification, which is in Appendix IV.

Three S-13 paints employing SP500 zinc oxide calcined at 650°C for 16 hr were irradiated in tests V-47 and V-56. The effects of the space-simulation tests on their solar absorptance are shown in Table 10. The SRC-05 catalyst concentration was 1 drop/35 grams of paint in all three cases. The nominal thickness of the two specimens for which aliphatic solvents were used (n-butanol and isooctane) was 4 mils. The nominal thickness of the specimen irradiated in test V-47 was 5 mils. The effect of calcination is manifest both in their initial α, which was only

IIT RESEARCH INSTITUTE

Table 10

EFFECT OF UV IRRADIATION IN VACUUM ON ZINC OXIDE-PIGMENTED
METHYL SILICONE ELASTOMER PAINTS (TEST V-56)

Sample	PVC, %	Pigment	Solvent	Exposure, ESH	Solar Absorptance			
					α_1	α_2	α	$\Delta\alpha$
S-13	30	Calcined SP500[a]	n-Butanol	0	.107	.089	.196	
				2100	.113	.091	.204	.008
S-13	30	Calcined SP500[a]	Isooctane	0	.105	.092	.197	
				2100	.117	.093	.210	.013
S-13	30	Calcined SP500[a]	Toluene	0	.095	.085	.180	
				2000[b]	.103	.095	.198	.018
Q92-002[c]	35	SP500	Xylene	0	.113	.109	.222	
				2100	.128	.110	.238	.016

[a]Calcined at 650°C for 16 hr.

[b]Test V-47 (Report No. IITRI-C6027-7).

[c]Furnished by Dow Corning; based on their proprietary RTV methyl silicone.

0.18 for the 5-mil coating, and the suggested improvement in $\Delta\alpha$, which was only 0.018 for the 5-mil coating.

Furthermore, these tests tend to confirm the improvement in stability noted in the Semiannual Report when toluene, used as the solvent in the standard S-13 formulation, was replaced by aliphatic solvents. Methyl silicone photolysis studies for Contract No. NAS8-5379 for NASA's George C. Marshall Space Flight Center have not shown this trend when the paint specimens are thoroughly cured and thermally evacuated before ultraviolet irradiation in vacuum. It is therefore thought that the choice of solvent is more critical when the specimens are to be irradiated soon after preparation and without aging at slightly elevated temperatures in vacuum. However, since it is difficult to thermally evacuate hardware larger than small satellites and spacecraft subassemblies, we believe the choice of the solvent must still be carefully considered. Further examination of this problem is indicated, and we are attempting to elucidate the role of solvent in conjunction with our silicone photolysis studies (ref. 4).

Additional data on S-13 coatings employing calcined SP500 zinc oxide and aliphatic solvents are presented in Section V-D.

The Q-92-002 specimen examined in test V-56. (Table 10) was furnished by Dow Corning Corporation. It is identical to specimen Q90-106 (described in IITRI Report No. IITRI-C207-25), except that it possesses a PVC of 35% compared with a PVC of 25% for the specimen examined earlier. The stability of Q92-002

IIT RESEARCH INSTITUTE

25

($\Delta\alpha$ = 0.016) is better than that of specimen Q90-106 ($\Delta\alpha$ = 0.033) for a nominal exposure of 2000 ESH. Although the S-13 coatings appear to be tougher and less easily scratched, Q92-002 compares very favorably with the S-13 system on the basis of the single test.

B. Adhesives for Detached S-13 Films

During the Semiannual Report period experiments were conducted to prepare wallpaper-like strips of precured, detached S-13 films that could be cemented to either a pressure-sensitive backing or a metal surface. Various methods of cementing the elastomeric S-13 film to aluminum substrates were explored. Test strips were prepared by using a Gardner knife to deposit a sufficiently thick film to provide a 10-mil dry film. The results are summarized in Table

Of the three potentially useful adhesives (GE SR585, GE 102, and DC Silastic 280), GE SP585 and Silastic 280 were evaluated in space-simulation tests. These results are presented in Table 12. In the first test, S-13 was cemented to an aluminum substrate with SR585 and soaked in vacuum overnight at 200°F before it was exposed to 1000 ESH of ultraviolet radiation (test V-48). Although the solar absorptance was not measured, the surface turned dark tan. In the second test, test V-47, the S-13/SR585 composite was subjected to 200 ESH of radiation (it was again thermally evacuated before exposure to ultraviolet). The degradation ($\Delta\alpha$ = 0.11) was attributed to the instability of the silicone adhesive, possible because

IIT RESEARCH INSTITUTE

Table 11

EFFECTIVENESS OF VARIOUS ADHESIVES FOR CEMENTING
S-13 FILMS TO ALUMINUM SUBSTRATES

Adhesive	Remarks
3M EC-226	Solvent-base hard-rubber adhesive. Very good adhesion to substrate. Test strip peeled off the adhesive very easily.
Bondmaster K218-34	Solvent-base medium-hard adhesive. Very good adhesion to substrate. Test strip peeled off the adhesive Very easily.
Dennis C-230-752-H	Solvent-base clear plastic adhesive. Very good adhesion to substrate. Test strip peeled off the adhesive very easily.
Fiber-reinforced contact pressure-sensitive adhesive	Adhesive strip applied from coated release paper. Good adhesion to substrate. Moderate adhesion of test strip.
GE SR585, experimental pressure-sensitive adhesive	Applied as thin film in toluene. Good adhesion to substrate. Good adhesion of test strip.
GE 102, moisture-cured silicone adhesive	Applied as a paste from a tube. Good adhesion to substrate. Adhesion improved by using SS-4044 silicone primer on substrate. Very good adhesion of test strip.
Dow Corning Silastic 280, pressure-sensitive adhesive	Applied as thin film in toluene. Good adhesion to substrate. Adhesion of test strip good.

27

of upward diffusion of low-molecular-weight aromatic and unsaturated materials in the adhesive during the vacuum/thermal soaking.

Table 12

UV DEGRADATION OF PREDETACHED S-13 PAINT FILMS

Sample	Adhesive	Test	Exposure, ESH	Solar Absorptance			
				α_1	α_2	α	$\Delta\alpha$
1	GE SR585	47	0	—	—	.240	
			2000	—	—	.350	.110
2	Silastic 280	51	0	.091	.107	.198	
			2000	.101	.108	.209	.011
3	Silastic 280	51	0	.088	.101	.189	
			2000	.101	.103	.204	.015
4	Silastic 280	51	0	.087	.100	.187	
			2000	.099	.099	.198	.011

Table 12 also shows the results of ultraviolet irradiation in vacuum on three specimens of predetached S-13 paint films that were bonded by Dow Corning Silastic 280 adhesive to aluminum substrates. The results of test V-51 show that the Silastic 280 adhesive had no effect upon the stability of the S-13 film to ultraviolet irradiation in vacuum.

C. S-33 and Synthesis of Experimental Methyl Silicone Resins

An experimental methyl silicone resin with an Me/Si ratio of about 1.4 and a molecular weight of 2300 showed excellent stability under simulated space conditions when prepared as a

IIT RESEARCH INSTITUTE

IITRI-C6027-16

zinc oxide-pigmented coating, S-33. Attempts to reproduce this resin gave products with molecular weights as low as 1600; some of these, compared to the original series, exhibited inferior stability to the simulated space environment.

Therefore the studies of the experimental methyl silicone resins planned for this program were intended to provide infor- mation required to prepare pilot quantities of stable resins with good physical properties. An additional task was the development of a satisfactory curing agent or cross-linking procedure for the experimental silicones. The curing agent used was 1% tetrabutoxy titanium based on silicone resin solids, and it is thought that a more satisfactory curing agent can be found in terms of the contribution to the instability that the cross-linking agent or the catalyst may impart to the paints.

Due to the discovery that the now available methyl silicone Glass Resins manufactured by Owens-Illinois possess exceptional stability to ultraviolet irradiation in vacuum, work on our experimental resin was limited to completion of studies on those resin batches prepared in the Semiannual Report period. Zinc oxide-pigmented Type 650 Owens-Illinois resins have not been observed to suffer an increase in solar absorptance after as much as 2000-ESH exposure to ultraviolet in vacuum. Indeed, they usually exhibit $\Delta\alpha$'s of about -0.005 on irradiation. The initial studies on these materials are being performed on another program (ref. 4). Cure studies

IIT RESEARCH INSTITUTE

IITRI-C6027-16

on the experimental methyl silicone polymers were therefore not undertaken.

Preparation of a typical resin has been reported in detail (ref. 6). The molecular weight and chemical analyses of resins with an Me/Si ratio of 1.4 molecularly distilled at various pressures and temperatures are presented in Table 13 (the initial condensation polymerizations were identical for the R-77 series).

The calculated analysis for a resin of the R77-type series and an Me/Si of 1.4 is: Si, 38.39; O, 31.96; C, 23.50; H, 6.15%. These values are based upon the following structural formula:

$$
\text{HO} - \left[\begin{array}{c} \underset{\underset{CH_3}{|}}{\overset{\overset{CH_3}{|}}{Si}} - O - \underset{\underset{OH}{|}}{\overset{\overset{CH_3}{|}}{Si}} - O - \underset{\underset{CH_3}{|}}{\overset{\overset{CH_3}{|}}{Si}} - O - \underset{\underset{CH_3}{|}}{\overset{\overset{CH_3}{|}}{Si}} - O - \underset{\underset{CH_3}{|}}{\overset{\overset{O}{|}}{Si}} - O - \underset{\underset{CH_3}{|}}{\overset{\overset{CH_3}{|}}{Si}} - O - \underset{\underset{O}{|}}{\overset{\overset{CH_3}{|}}{Si}} - O - \right]_5 \text{H}
$$

which has a molecular weight of 2553 and an Me/Si of 1.43. The chemical analyses reported in Table 13 were performed by Schwarzkopf Microanalytical Laboratory, who analyzed for Si, C, and H. The excellent agreement between resins R77-2, -3 and -6 is heartening; it is indicative of good repeatability by utilizing the polymerization scheme outlined previously (ref. 6).

Several molecularly distilled methyl silicone resins were formulated into paints at 30% PVC by using SP500 zinc oxide and 1% tetrabutoxy titanium (based on resin solids) as the crosslinking agent. Solvents for these paints were toluene and butanol. Since no attempt was made to minimize them, the initial

IIT RESEARCH INSTITUTE

Table 13

ANALYSIS AND MOLECULAR WEIGHT OF METHYL SILICONE RESINS
AFTER MOLECULAR DISTILLATION (HIGH-BOILING FRACTIONS)

Resin	Distillation Conditions		Molecular Weight	Analysis, %				
	Pressure, torrs	Temp., °C		Me/Si	Si	O	C	H
R77-2	0.3	150-160	2350	1.40	38.15	32.85	22.89	6.11
R77-3	0.02	135-150	2100	1.47	37.08	33.24	23.31	6.37
R77-6	0.005	150	3050	1.43	38.29	32.21	23.37	6.13
R77-18	0.005	150	2400	–	–	–	–	–
R77-20	0.005	150	2575	–	–	–	–	–

solar absorptances of these paints are rather high. The effects
of ultraviolet irradiation in vacuum are shown in Table 14 (test
V-54). The only conclusion that could be reached was that all
of the experimental resin-based paints were more stable optically
than the S-13 paints irradiated in the same test.

Table 14

UV DEGRADATION OF MOLECULARLY DISTILLED METHYL SILICONE RESINS
PIGMENTED WITH ZnO SP500 AT 30% PVC (Me/Si = 1.4)

Sample	In Toluene		In Butanol	
	α	$\Delta\alpha$	α	$\Delta\alpha$
R77-5[a]	.252	.036	.314	.034
R77-6B	.245	.038	.270	.034
R77-18			.250	.042
R77-20			.244	.036

[a]Me/Si = 1.3.

However, all paints irradiated in test V-54 exhibited un-
usually large $\Delta\alpha$'s. This is attributed to the fact that the
specimens in test V-54 were not thermally evacuated before
irradiation and that several of the adjacent S-13 coatings were
probably not sufficiently cured. Therefore, it is believed that
some unreacted amine catalyst, SRC-05, photolyzed as a varnish
upon many of the specimens.

Other specimens of paints prepared from the experimental
resins were subjected to 2000 ESH of ultraviolet radiation in
test V-56. The results of this test are presented in Table 15.

IIT RESEARCH INSTITUTE

32

Table 15

EFFECT OF UV IRRADIATION IN VACUUM ON ZINC OXIDE-PIGMENTED
EXPERIMENTAL METHYL SILICONE RESINS (TEST V-56)

Sample	Resin	Nominal Me/Si	PVC, %	Solvent	Exposure, ESH	Solar Absorptance			
						α_1	α_2	α	$\Delta\alpha$
5004	R54-3A	1.6	30	Isooctane	0	.102	.130	.232	
					2100	.104	.131	.235	.003
5005	R54-3A	1.6	30	Methanol	0	.109	.135	.244	
					2100	.114	.137	.251	.007
5006	R54-3A	1.6	40	n-Butanol	0	.094	.103	.197	
					2100	.096	.104	.200	.003
5008	R54-7A[a]	1.6	30	Toluene	0	.097	.112	.209	
					2100	.099	.113	.212	.003
5012B	R54-6B	1.4	30	n-Butanol	0	.115	.147	.262	
					2100	.115	.148	.263	.001
5013B	R54-9[b]	1.4	30	n-Butanol	0	.089	.086	.175	
					2100	.090	.086	.176	.001

[a]This was the only resin in the series R54 that was passed through activated carbon.
[b]This is the low-boiling fraction from molecular distillation.

Specimens 5004 through 5006 are based on resin R54-3A at an Me/Si ratio of 1.6 (calculated from di- and tri-functional chlorosilane reactants). Resin R54-7A is identical to R54-3A except that it was passed through activated carbon.

Sample 5012B was a repeat from test V-54, in which it suffered an increase in solar absorptance of 0.034. As noted above, this discrepancy is believed to be due to contamination during test V-54. However, the results of test V-56 again confirm the inherent stability of the methyl silicone resin paints especially when prepared at lower Me/Si ratios.

Sample 5013B was prepared from the low-boiling fraction after molecular distillation of a resin with an Me/Si of 1.4. It is interesting to note that, as in all previous paints prepared from low-boiling fractions, the solar absorptance of the paint is a comparatively low 0.175.

The specimens in test V-56 were thermally soaked in vacuum for about 16 hr before irradiation. Furthermore, no difference was discerned between the specimens that employed toluene and those that employed isooctane and n-butanol.

V. SIMULATION PARAMETERS

A. High-Temperature Irradiation Tests

In three high-temperature, ultraviolet-exposure tests (in vacuum) of silicate paints at 425, 500, and 610°F, we obtained differential reflectance plots that are typified by the curves presented in Figure 2. The silicate paints consisted of three SP500 zinc oxide-pigmented coatings and one zirconia-potassium silicate paint. The PBR's of the zinc oxide-potassium silicate paints were 2.15, 4.30 (Z93 specification paint), and 6.45. The PBR of the zirconia paint was 4.30.

In each test all samples were exposed to the same temperatures but only half were exposed to ultraviolet radiation

The solar absorptance before and after exposure to the combined temperature and ultraviolet and to temperature alone for each temperature are presented in Table 16.

Perhaps the most outstanding feature of the degradation data is the similarity of the ΔR_λ curves (Figure 2). The trends are all as would be predicted; e.g., ultraviolet plus temperature produces more damage than temperature alone; higher temperatures lead to greater damage; and higher PBR's are, in general, more stable from an optical point of view.

Because these tests were performed in a 10-in. oil diffusion-pumped system and because the damage seems higher than would be predicted from previous data, we are skeptical of the quantitative aspects of the results. Although oil contamination may have been responsible for the generally high $\Delta\alpha$'s observed,
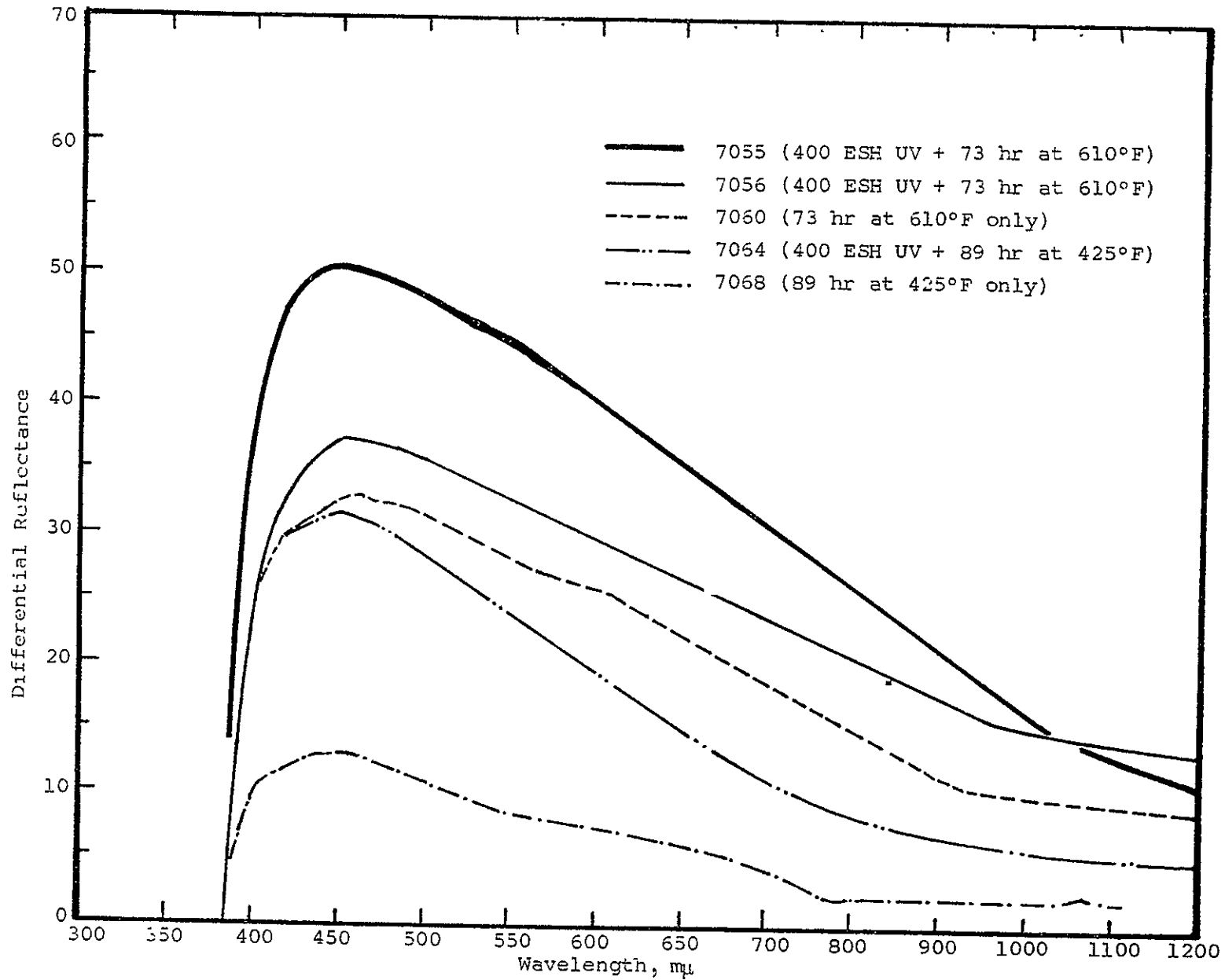
IIT RESEARCH INSTITUTE

35

Figure 2

DIFFERENTIAL REFLECTANCE SPECTRA OF SILICATE PAINTS IRRADIATED AT HIGH TEMPERATURES

Table 16

EFFECT OF UV IRRADIATION IN VACUUM ON SILICATE PAINTS
AND ZIRCONIA AT ELEVATED TEMPERATURES

Composition						Solar Absorptance			
Pigment	PBR	Sample	Temp., °F	Exposure, ESH	Hours at Temp.	α_1	α_2	α	$\Delta\alpha$
SP500 ZnO	6.45	7062	425	0		.091	.069	.160	
		7062U	425	400		.182	.085	.267	.107
		7066	425	.	0	.091	.074	.165	
		7066T	425		89	.127	.080	.207	.042
		7080	500	0		.086	.032	.118	
		7080U	500	440		.224	.064	.288	.170
		7081	500		0	.097	.047	.144	
		7081T	500		88	.137	.060	.197	.053
		7054	610	0		.093	.075	.168	
		7054U	610	400		.221	.145	.366	.198
		7058	610		0	.092	.074	.166	
		7058T	610		77	.150	.095	.245	.079
SP500 ZnO	4.30	7064	425	0		.101	.090	.191	
		7064U	425	400		.198	.111	.309	.118
		7068	425			.104	.098	.202	
		7068T	425		89	.141	.103	.244	.042
		7084	500	0		.097	.067	.164	
		7084U	500	440		.232	.071	.303	.139
		7085	500		0	.089	.046	.135	
		7085T	500		88	.137	.061	.198	.063
		7056	610	0		105	.100	.205	
		7056U	610	400		245	.166	.411	.206
		7060	610		0	101	.095	.196	
		7060T	610		73	219	.137	.356	.160
SP500 ZnO	2.15	7063	425	0		152	.192	.344	
		7063U	425	400		268	.194	.462	.118
		7067	425		0	.143	.199	.342	
		7067T	425		89	.171	.173	.344	.002
		7082	500	0		.142	.152	.294	
		7082U	500	440		.255	.141	.396	.102
		7083	500		0	.123	.153	.276	
		7083T	500		88	.145	.113	.258	−.018
		7055	610	0		.139	.197	.337	
		7055U	610	400		.339	.246	.585	.248
		7059	610		0	.144	.202	.346	
		7059T	610		73	.268	.201	.469	.123
ZrO$_2$	4.30	7065	425	0		.084	.137	.221	
		7065U	425	400		.290	.182	.472	.251
		7069	425		0	.076	.127	.203	
		7069T	425		89	.116	.125	.241	.038
		7086	500	0		.087	.099	.186	
		7086U	500	440		.276	.128	.404	.218
		7087	500		0	.072	.099	.171	
		7087T	500		88	.126	.098	.224	.053
		7057	610	0		.072	.126	.198	
		7057U	610	400		.332	.218	.550	.352
		7061	610		0	.097	.151	.247	
		7061T	610		73	.258	.164	.422	.175

the data in Table 16 nevertheless indicate that it appears not to have affected the underlying degradation processes -- at least as manifest in the spectral reflectance changes.

Other conclusions should not be drawn from the data, since, when examined, the samples usually showed markedly nonuniform effects. It is not known whether these effects resulted from contamination due to back-diffusion of pump oil or inhomogeneities in the sample.

Previous studies (ref. 6) showed that damage at low temperatures (-300°F) was less than at room temperature. These same data showed that both zinc oxide-pigmented methyl silicone and potassium silicate paints degrade more severely at 200°F than at room temperature. S-13 specimens exhibited $\Delta\alpha$'s of 0.05 and Z93 exhibited $\Delta\alpha$'s of 0.03 after 1040 ESH (4.6 suns). These data are reproduced in Tables 17 and 18, taken from the earlier report.

The lower solar absorptances reported in Table 16 for the 500°F test are the result of data obtained with the Beckman DK-2A spectroreflectometer. Values reported for the other temperatures were calculated from Cary 14 reflectance measurements. The differences, which are about 0.04 to 0.05, are due to the Vitro-lite standard, which gives differences between the two instruments of the same magnitude.

B. Intensity-Dependence (Reciprocity) Experiments

The need for information relating ultraviolet radiation-induced damage to the quantity of radiation producing it in space simulation brings up questions of the validity of accelerated

IIT RESEARCH INSTITUTE

38

Table 17

EFFECT OF TEMPERATURE AND INTENSITY ON THE UV DEGRADATION RATE
OF THERMAL-CONTROL COATING S-13 IN THE QUAD-ION SYSTEM

Sample[a]	Test No.	Substrate Temp., °F	Exposure		Solar Absorptance			
			ESH	Solar Factor	α_1	α_2	α	$\Delta\alpha$
1-TC	Q1	43	0		.096	.106	.202	
			1020	5.1	.130	.089	.219	.017
2-TC	Q1	43	0		.084	.090	.174	
			1020	5.1	.126	.087	.213	.039
3	Q3	200	0		.086	.090	.175	
			1040	4.6	.101	.108	.209	.034
4	Q3	200	0		.085	.087	.172	
			1040	4.6	.115	.112	.226	.054
5M-TC	Q4	-306	0		.088	.091	.179	
			1170	4.9	.094	.092	.186	.007
6M-TC	Q4	-306	0		.088	.094	.182	
			1170	4.9	.092	.095	.187	.005
7M	Q4	195	0		.090	.110	.200	
			1100	11.1	.096	.106	.202	.002
8M	Q4	195	0		.089	.100	.189	
			1100	11.1	.093	.111	.204	.015
9M	Q5	40	0		.091	.106	.197	
			1000	23.2	.092	.105	.197	.000
S-33	Q5	40	0		.127	.148	.275	
			1000	23.2	.136	.150	.286	.011

[a]Samples designated TC had thermocouples imbedded in the coating.
Samples designated M were cured with half the usual
concentration of SRC-05 catalyst.

Table 18

EFFECT OF TEMPERATURE AND INTENSITY ON THE UV DEGRADATION RATE
OF THERMAL-CONTROL COATING Z93 IN THE QUAD-ION SYSTEM

Sample[a]	Test No.	Substrate Temp., °F	Exposure ESH	Solar Factor	Solar Absorptance α_1	α_2	α	$\Delta\alpha$
1-TC	Q1	43	0		.088	.071	.159	
			1020	5.1	.102	.068	.170	.011
2-TC	Q1	43	0		.088	.071	.159	
			1020	5.1	.100	.066	.166	.007
3-TC	Q3	200	0		.083	.074	.157	
			1040	4.6	.114	.076	.190	.033
4-TC	Q3	200	0		.084	.074	.158	
			1040	4.6	.113	.074	.187	.029
5	Q3	5	0		.084	.074	.157	
			1020	8.6	.092	.069	.161	.004
6	Q3	5	0		.083	.073	.156	
			1020	8.6	.091	.068	.159	.003
7-TC	Q4	-292	0		.088	.076	.164	
			1170	4.9	.089	.074	.163	-.001
8	Q4	-292	0		.084	.071	.155	
			1170	4.9	.085	.070	.155	.000
9	Q4	195	0		.083	.071	.156	
			1100	11.1	.099	.067	.166	.010
10	Q4	195	0		.082	.067	.149	
			1100	11.1	.099	.065	.164	.015
11-TC	Q5	160	0		.088	.076	.164	
			1000	23.2	.095	.075	.170	.006
12	Q5	160	0		.083	.069	.152	
			1000	23.2	.087	.069	.155	.003

[a]Samples designated TC had thermocouples imbedded in the coating.

IITRI-C6027-16

testing. The basis of accelerated ultraviolet testing has been (by assumption) that reciprocity holds for high intensity irradiation, implying that the Δa's induced by ultraviolet radiation are dependent only upon total dose received and not upon dose rate.

Test Q-8 was performed in the Quad-Ion facility in order to determine the relation between intensity and damage for equivalent exposures. Chambers I and II contained identical specimens of S-13 and S-33; chambers III and IV contained identical specimens of Z93 and a zirconia-silicate paint. Chambers I and III received 1020 ESH of ultraviolet radiation at 3.9 solar intensities; chambers II and IV received 1250 ESH at 14.4 solar intensities. All specimens were epoxied to a cooled sample table maintained at 41°F.

The results of test Q-8 are presented in Table 19. The experimental methyl silicone-based coating, S-33, was the only coating that responded similarly to specimens previously irradiated at high intensity. That is, S-33 exhibited an apparent inverse dependence of damage upon intensity such that less damage was produced at the higher radiation level. This is even more pronounced when considering the fact that the 14.4-sun test was for 230 more ESH exposure than the 3.9-sun exposure.

The validity of test Q-8 is demonstrated by the 0.056 increase in solar absorptance exhibited by the zirconia specimen. The companion specimen irradiated at the higher intensity exhibited a direct intensity dependence since it degraded 0.133 at the 14.4-sun intensity.

41

Table 19

EFFECT OF UV IRRADIATION INTENSITY
ON THE SOLAR ABSORPTANCE OF THREE SPECIFICATION COATINGS
AND ZIRCONIA (1000 ESH, TEST Q-8).

| Sample | Coating | Exposure | | Solar Absorptance | | | |
		Solar Intensity	ESH	α_1	α_2	α	$\Delta\alpha$
5012-1C	S-33[a]	0	0	.095	.105	.200	
		3.9	1020	.101	.114	.215	.015
5012-2C	S-33[a]	0	0	.094	.105	.199	
		14.4	1250	.101	.105	.206	.007
5068-1	S-13	0	0	.078	.056	.134	
		3.9	1020	.090	.061	.151	.017
5068-2	S-13	0	0	.078	.058	.136	
		14.4	1250	.099	.060	.159	.023
7088	Z93	0	0	.077	.036	.114	
		3.9	1020	.088	.036	.124	.010
7089	Z93	0	0	.076	.036	.112	
		14.4	1250	.094	.032	.126	.014
7090	Zirconia	0	0	.061	.096	.157	
		3.9	1020	.118	.095	.213	.056
7091	Zirconia	0	0	.062	.096	.158	
		14.4	1250	.195	.096	.291	.133

[a]Contained butyl alcohol as the solvent.

IITRI-C6027-16

Although the higher-intensity test for S-13 and Z93 exhibited slightly greater damage than the lower-intensity exposures, the 20% greater total exposure (dose) at the 14.4-sun level makes these data consistent with those reported in the Semiannual Report. The data on temperature and intensity effects reported in Report No. IITRI-C6027-7 are reproduced as Tables 17 and 18.

The data in Tables 17 through 19 show that the behavior of the silicone paints S-13 and S-33 is similar to that of the inorganic silicate paint Z93. Furthermore, it must be concluded that the sensitivity of a given coating system must be evaluated before accelerated testing. That is, although it appears that S-13 and Z93 are relatively insensitive to intensity between 5 and 15 solar factors (and at worst, exhibit a mild inverse dependence on intensity), zirconia is definitely more sensitive to higher-intensity irradiation and reciprocity does not appear to hold for this coating. On the other hand, the S-33 coating exhibited a mild inverse dependence on irradiation level (Table 19), as did both S-13 and Z93 at the very high solar intensity of 23 suns (Tables 17 and 13).

The inverse dependency noted is in direct contrast to the observations reported in Report No. IITRI-C207-27; namely, at the higher intensities the damage was more severe, not less. However, the increased damage at the higher intensities in the earlier work is attributed to thermal effects associated with the high-intensity accelerated testing when not accompanied by substrate cooling. The specimens reported in the present

IIT RESEARCH INSTITUTE

43

studies were epoxied to the cooled sample table.

The important observation from this work is that the reciprocity theorem may or may not hold, and the degree to which it does is highly specific.

C. Filtered-Ultraviolet-Radiation Experiments

The initial filter experiment, test 48, was conducted early in the program and was discussed in the Semiannual Report. Filter experiments were undertaken to determine, if possible, the wavelengths of radiation that are most damaging to the three specification thermal-control coatings (Z93, S-13, and S-33) and to ascertain the adequacy of the AH-6 lamp in simulating the effects of extraterrestrial ultraviolet radiation.

Although difficulty was experienced in test 48 as a result of excessive filter degradation, it was suggested that visible light may bleach ultraviolet-induced visible absorption bands or bands that fall into the visible region of the spectrum. This speculation was based on the greater increase in solar absorptance that occurred under filter 7-51 (in that test) compared with the increase under filter 7740, which transmitted considerably more ultraviolet (also of more energetic wavelengths) as well as visible light.

Filter experiments were therefore planned for the Quad-Ion space-simulation facility so that the extent of bleaching of induced absorption bands by visible light could be ascertained and the validity and degree of space simulation by the AH-6 lamp

could be determined. In test Q-6, a Corning 7-54 glass filter was used in an assembly resembling that depicted in Figure 16 in Appendix V. After several days of operation the filter assembly degraded to the extent that insufficient ultraviolet energy was transmitted, so test Q-6 was terminated. (The effect of 1 hr of ultraviolet irradiation in air on the transmittance of 7-54 filter glass is presented in Figure 13 in Appendix V).

The 7-54 filter degradation problem prompted the development of a liquid filter that would not exhibit serious decreases in transmittance during a test. The filter system developed is discussed in detail in Appendix V. The filter solution is an acidified (H_2SO_4) mixture of cobalt and nickel sulfate, which exhibits a long-wavelength cutoff at 3600 A and a short-wavelength cutoff at 2200 A. The transmittance spectra of the liquid-filter assembly is presented in Figure 3.

Because the liquid filter possesses a cutoff at 2200 A, a Corning 7910 glass filter, which also has a 2200-A cutoff but which transmits visible light, was used in the next filter test (test Q-9). Thus it was thought that the differences in ultraviolet radiation received by both sets of samples would be minimized by excluding radiation below 2200 A from both sets. The transmittance spectra of the 7910 filter are also presented in Figure 3.

The samples were exposed to two different irradiation spectra; the radiation schedule is presented in Table 20. Note that the unfiltered spectrum contains approximately 30% more ultraviolet than the filtered spectrum.
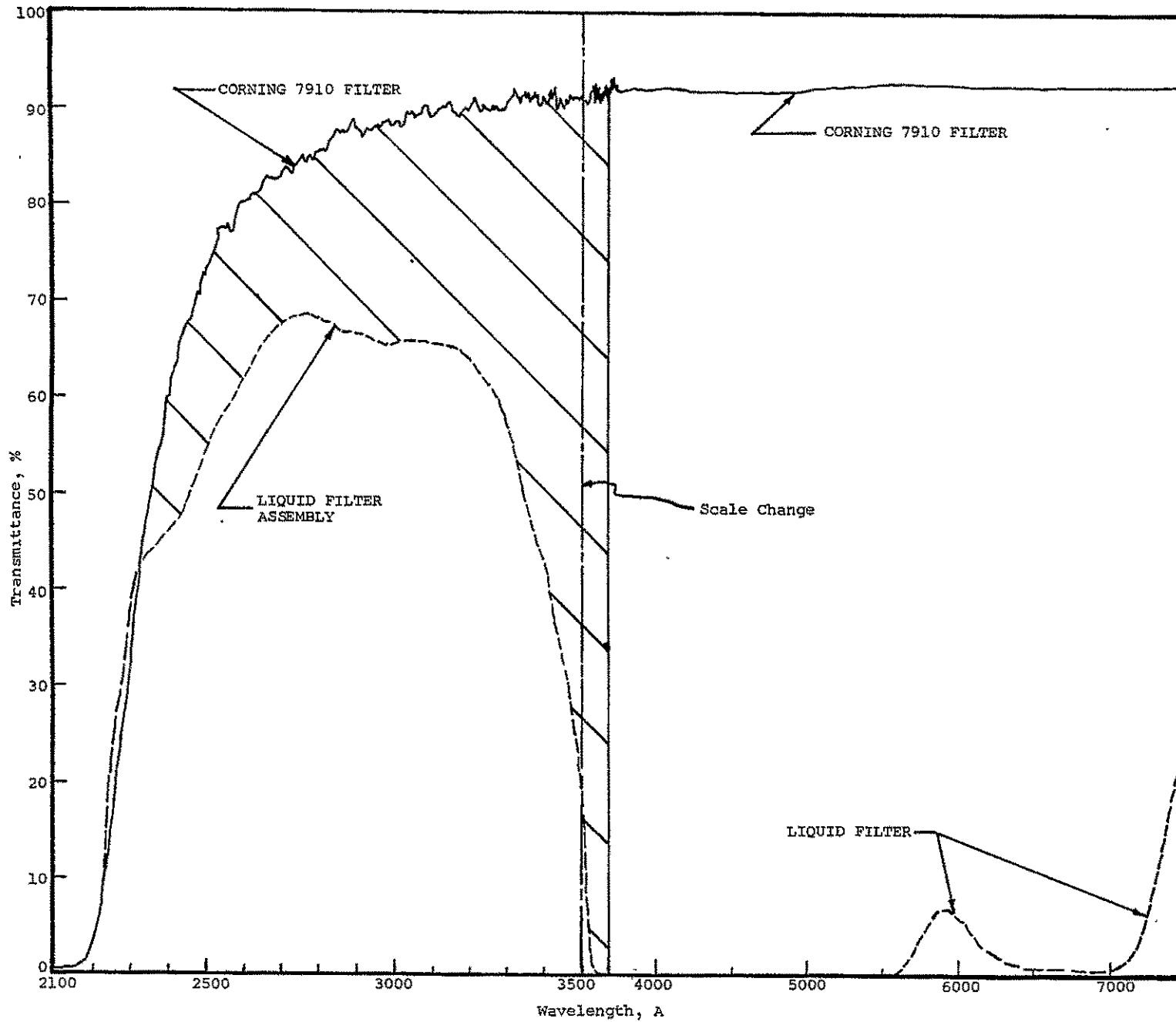
Figure 3

TRANSMITTANCE OF FILTER ASSEMBLIES USED IN TEST Q-8

Table 20

SCHEDULE OF FILTERED UV RADIATION EXPERIMENT (TEST O-9)

No.	Sample Description	Liquid Filter 2200-3600 A	Corning 7910 Filter $\lambda > 2200$ A	Chamber I	II	III	IV	Remarks
5086	DC 808 resin film	X		X				
5087	DC 808 resin film		X		X			
5088	LTV-602/SRC-05 film	X		X				
5089	LTV-602/SRC-05 film		X		X			
5090	LTV-602/SRC-05/toluene	λ		X				Differential spectra = 5088.
5091	LTV-602/SRC-05/toluene		X		X			Differential spectra = 5089.
5092	S-13	X		X				
5093	S-13		X		X			
7018	Zinc oxide compact	X					X	Differential spectra not presented.
7019	Zinc oxide compact		X			X		
7114	Z93	X					X	
7115	Z93		X			X		
7116	Potassium silicate	X					X	Cracked; after T_λ not measured.
7117	Potassium silicate	X	X			X		Cracked; after T_λ not measured.

The silicone samples were prepared on quartz substrates in thin slices ($\sim$1/32 in. thick). The initial transmittance of all silicone films was in the range 90 to 95% in the visible and near-ultraviolet regions of the spectrum.

The Dow Corning 808 film is a phenyl-methyl silicone resin that was heat-cured. LTV-602, a 100% methyl silicone resin, was cured by an amine catalyst, SRC-05, which is proprietary to the General Electric Company.

The two materials exhibited somewhat different effects (Figure 4). The approximately 15% greater damage to the LTV-602 film in the unfiltered versus the liquid-filtered case must relate to the approximately 30% difference in total ultraviolet dose (exposure). The difference between the differential spectra exhibited by the LTV-602 (transmittance) and the S-13 thermal-control paint (reflectance) is attributed to the zinc oxide pigment, which absorbs all radiation below 3900 A.

On the other hand, at present we have only a tentative explanation for the behavior of Dow Corning 808, which, unlike that of the LTV-602, exhibited less damage in the ultraviolet portion of the spectrum (and more damage in the visible region) when irradiated with the entire spectrum (through the 7910 filter). The DC 808 data suggest that the ΔT_λ spectrum comprises two defect systems, which, when added together, produce the spectrum observed. The data thus show that the longer wavelength band is more strongly bleached by the greater intensity under the 7910 filter at the longer wavelength.

IIT RESEARCH INSTITUTE

48
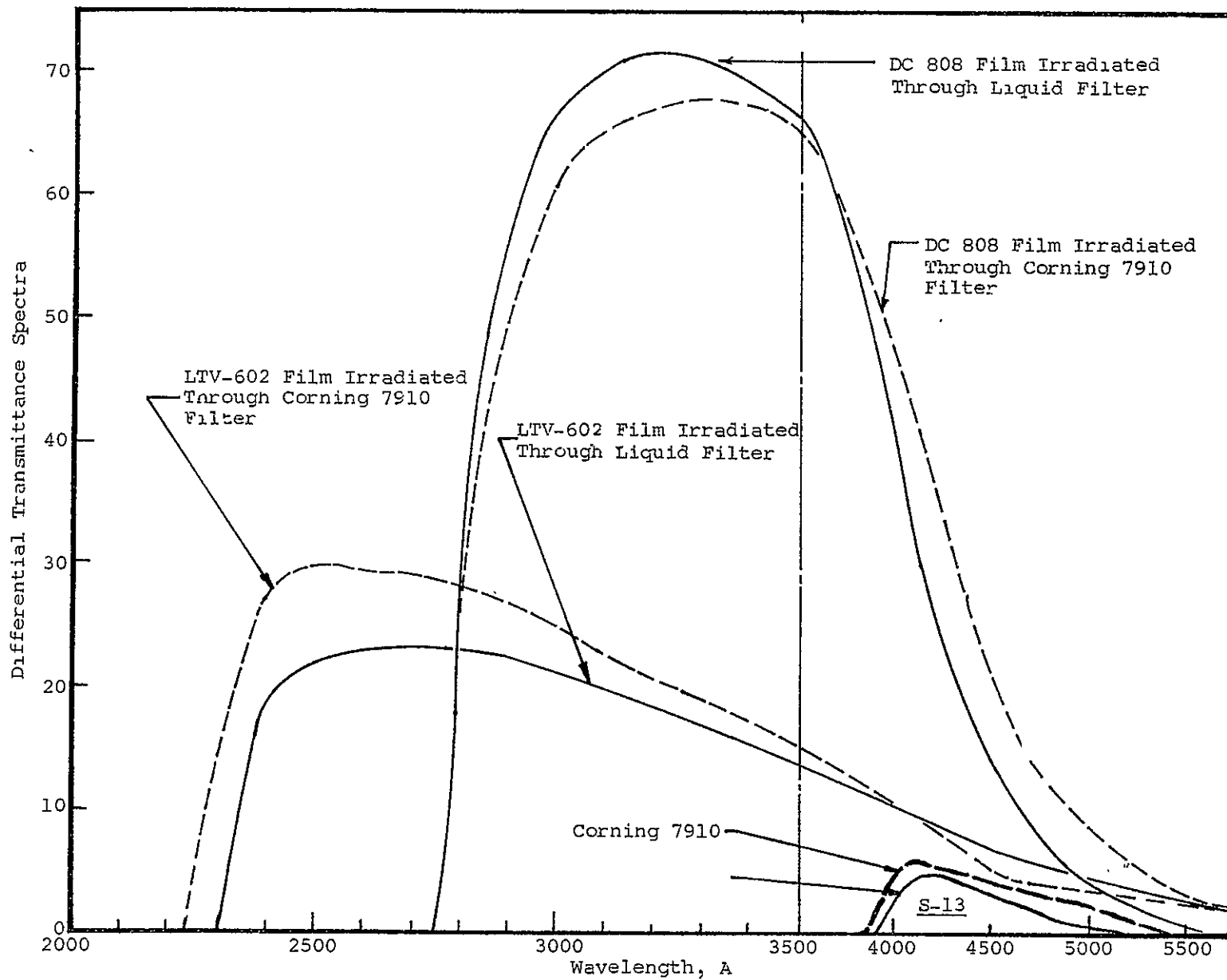
Figure 4

DIFFERENTIAL SPECTRA OF SILICONE FILMS DUE TO FILTERED UV

However, if the ΔT_λ curves representing the effects on samples irradiated by the entire spectrum were normalized to account for the additional ultraviolet energy they received, the two LTV-602 curves would more nearly coincide and the corresponding ΔT_λ curves for the DC 808 might differ still more greatly. Indeed, the ΔT_λ curve for 808 representing irradiation with the entire spectrum might then also be considerably less than the curve representing irradiation through the liquid filter. To further speculate, since the DC 808-induced absorption band, which falls into the visible portion of the spectrum (at wavelengths longer than 4000 A), is considerably more intense than that for LTV-602, it might be concluded that "bleaching" or color-center annihilation indeed occurs simultaneously with color-center formation. The color centers are presumably free radical in nature.

One of the criticisms of the AH-6 lamp has been its unrealistically high percentage of ultraviolet (~35%) compared to that in extraterrestrial sunlight (9%). The data shown in Figure 4 indicate that, although the visible component of incident radiation may play a part in the equilibrium process between formation and annihilation of color centers, the degradation quite obviously depends much more sensitively on the total ultraviolet exposure than on the spectral character of the irradiation spectrum. We therefore conclude that, from the standpoint of its use in irradiation of our three specification paints, the AH-6 lamp does not present a problem relative to its high percentage of ultraviolet and that it adequately simulates the effects of extraterrestrial

solar radiation in this respect. Furthermore, the high percentage of ultraviolet makes the AH-6 an ideal source for accelerated testing.

In the same experiments we irradiated zinc oxide as a compact and in the Z93 and S-13 paint compositions. The important conclusion, obtained from analyses of differential reflectance spectra, is that the damaged spectra are qualitatively identical. The zinc oxide-compact differential spectra are not shown since so little damage was observed. Accurate differential data could not be drawn without normalizing the reflectance values to account for different values obtained with the Vitrolite standard before and after irradiation. The spectra for S-13, which was also measured in reflectance, are presented; the degradation was sufficient to obtain valid differential curves.

The LTV-602 films containing toluene display degradation essentially identical to that of uncured films containing no solvent; they were therefore not shown. Although we have discussed the possibility that residual aromatic solvents play a role in photolysis of silicones, these results are inconclusive, since the specimens were thoroughly soaked in vacuum at approximately 200°F for 16 hr before irradiation. It is therefore thought that the concentration of any toluene present would have been insufficient to have an effect even if it does play a role in photolysis. Studies pertaining to silicone photolysis are being carried out under Contract NAS8-5379 with the George C. Marshall Space Flight Center (ref. 4).

D. The Effect of Exposure on Solar Absorptance (Long-Term Tests)

Samples of IITRI's three specification coatings (S-13, S-33 and Z93) as well as modifications of S-13 and Z93 were irradiated at about 6 solar intensities for several different exposures in tests Q-10, Q-11, and Q-12. These tests were performed in the Quad-Ion facility for 7900, 300, and 4500 ESH, respectively. The results of these tests are presented in Tables 21, 22, and 23. The data for S-13, S-33, and S-34 are plotted in Figure 5; the data for Z93, Z94, and the zirconia control sample are plotted in Figure 6.

The results of these tests, particularly the 7900-ESH exposure, were surprising; we did not expect the S-13 specimens to exhibit such exceptional stability. Furthermore, the greater severity of the 7900-ESH test on the alkali silicate paints was also unexpected. This severity is depicted more clearly in Figure 6, in which $\Delta\alpha$ is plotted as a function of the log of exposure. By contrast, the silicone paints shown in Figure 5 exhibit little difference in $\Delta\alpha$ when irradiated for 7900 ESH compared with 4500 ESH.

Differences in irradiation levels as a result of contamination of the window used to irradiate the silicone specimens has been ruled out, since (1) the window exteriors were cleaned at regular intervals during the tests and (2) the transmittances of all four windows indicated that residues were not deposited on the interior surfaces.

IIT RESEARCH INSTITUTE

52

Table 21

EFFECT OF 300 ESH UV IRRADIATION IN VACUUM ON SPECIFICATION COATINGS (TEST Q-11)

Sample	Coating	Treatment	Exposure, ESH	Solar Absorptance			
				α_1	α_2	α	$\Delta\alpha$
5012-C3-2	S-33	Experimental resin R-9 in n-butanol.	0	.093	.105	.198	
			300	.093	.106	.199	.001
5094-2	S-13	1 drop SRC-05/35 g of paint.	0	.097	.096	.193	
			300	.098	.096	.194	.001
5095-2	S-13	2 drops Shell H-2/35 g of paint.	0	.098	.083	.191	
			300	.098	.091	.189	-.002
5096-2	S-34	Modified S-13; calcined SP500 at 40% PVC, n-butanol, and SRC-05 at 1 drop/20 g.	0	.109	.081	.190	
			300	.105	.081	.186	-.004
7135	Z93	Prepared fresh.	0	.088	.059	.147	
			300	.092	.058	.150	.003
7136	Z93	4 months old.	0	.079	.043	.120	
			300	.083	.042	.125	.005
7137	Z93	4 months old.	0	.085	.053	.138	
7137HT	Z93	Heat-treated 2 hr at 500°C.	0	.081	.038	.119	
			300	.085	.039	.124	.005
7138	Z94	PBR = 6.45; 5 months old.	0	.092	.046	.138	
			300	.092	.043	.135	-.003
7139	Zirconia	PBR = 6.45; 4 months old.	0	.051	.054	.104	
			300	.083	.053	.136	.032

Table 22

EFFECT OF 4500 ESH UV IRRADIATION IN VACUUM ON SPECIFICATION COATINGS (TEST Q-12)

Sample	Coating	Treatment	Exposure, ESH	Solar Absorptance			
				α_1	α_2	α	$\Delta\alpha$
5012-C3-3	S-33	Experimental resin R-9 in n-butanol.	0 4500	.096 .109	.100 .102	.196 .211	 .015
5107	S-13	1 drop SRC-05/35 g of paint.	0 4500	.095 .118	.090 .092	.185 .210	 .025
5108	S-13	2 drops Shell H-2/20 g of paint.	0 4500	.094 .136	.080 .084	.174 .220	 .046
5106	S-13	2 drops Shell H-2/35 g of paint.	0 4500	.094 .114	.102 .102	.196 .216	 .020
5096-3	S-34	Modified S-13; calcined SP500 at 40% PVC, n-butanol, and SRC-05 at 1 drop/20 g.	0 4500	.125 .133	.113 .110	.238 .245	 .005
7140	Z93	Prepared fresh.	0 4500	.089 .120	.061 .054	.150 .174	 .024
7141	Z93	4 months old.	0 4500	.084 .111	.049 .046	.133 .157	 .024
7142 7142HT	Z93	4 months old. Heat-treated 2 hr at 500°C.	0 0 4500	.082 .084 .107	.049 .042 .045	.131 .126 .152	 .026
7143	Z94	PBR = 6.45; 5 months old.	0 4500	.091 .117	.053 .046	.144 .163	 .019
7144	Zirconia	PBR = 6.45; 4 months old.	0 4500	.066 .187	.064 .060	.130 .247	 .117

Table 23

EFFECT OF 7900 ESH UV IRRADIATION IN VACUUM ON SPECIFICATION COATINGS (TEST Q-10)

Sample	Coating	Treatment	Exposure, ESH	Solar Absorptance			
				α_1	α_2	α	$\Delta\alpha$
5012-C3	S-33	Experimental resin R-9 in n-butanol.	0	.102	.117	.219	
			7900	.116	.116	.232	.013
5094-1	S-13	1 drop SRC-05/35 g of paint.	0	.092	.095	.187	
			7900	.117	.096	.213	.026
5095-1	S-13	2 drops Shell H-2/35 g of paint.	0	.091	.095	.186	
			7900	.113	.096	.209	.023
5096-1	S-34	Modified S-13; calcined SP500 40% PVC, n-butanol, and SRC-05 at 1 drop/20 g.	0	.103	.086	.189	
			7900	.122	.084	.206	.017
7130	Z93	Prepared fresh; PBR = 4.3.	0	.090	.060	.150	
			7900	.139	.060	.199	.049
7131	Z93	4 months old.	0	.080	.044	.124	
			7900	.126	.044	.120	.046
7132	Z93	4 months old.	0	.084	.056	.140	
7132HT	Z93	Heat-treated 2 hr at 500°C.	0	.083	.036	.119	
			7900	.127	.045	.172	.053
7133	Z94	PBR = 6.45; 5 months old.	0	.089	.050	.139	
			7900	.137	.050	.187	.040
7134	Zirconia	PBR = 6.45; 4 months old.	0	.049	.050	.099	
			7900	.261	.072	.333	.234
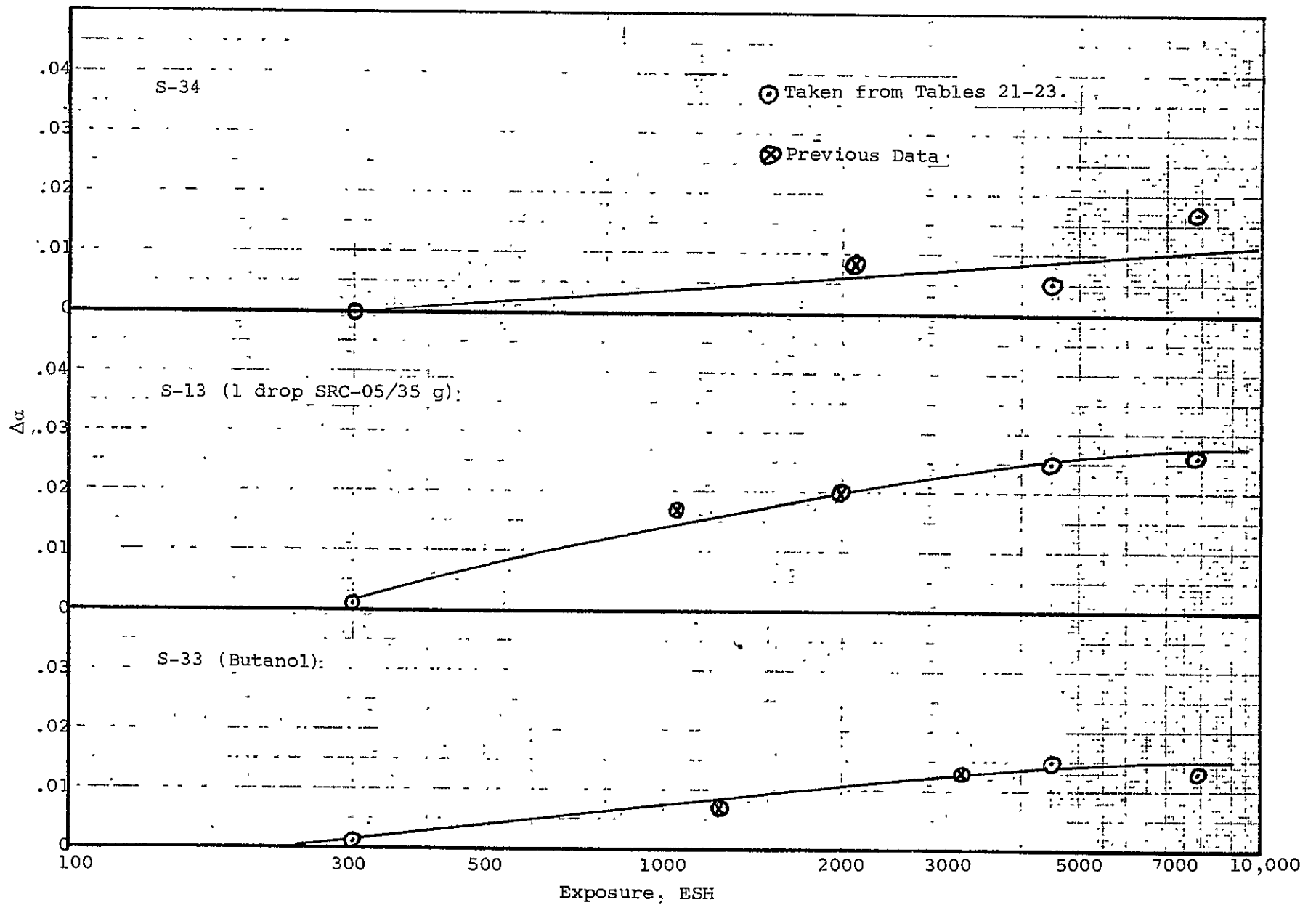
Figure 5

INCREASE IN SOLAR ABSORPTANCE OF SILICONE PAINTS AS A FUNCTION OF EXPOSURE
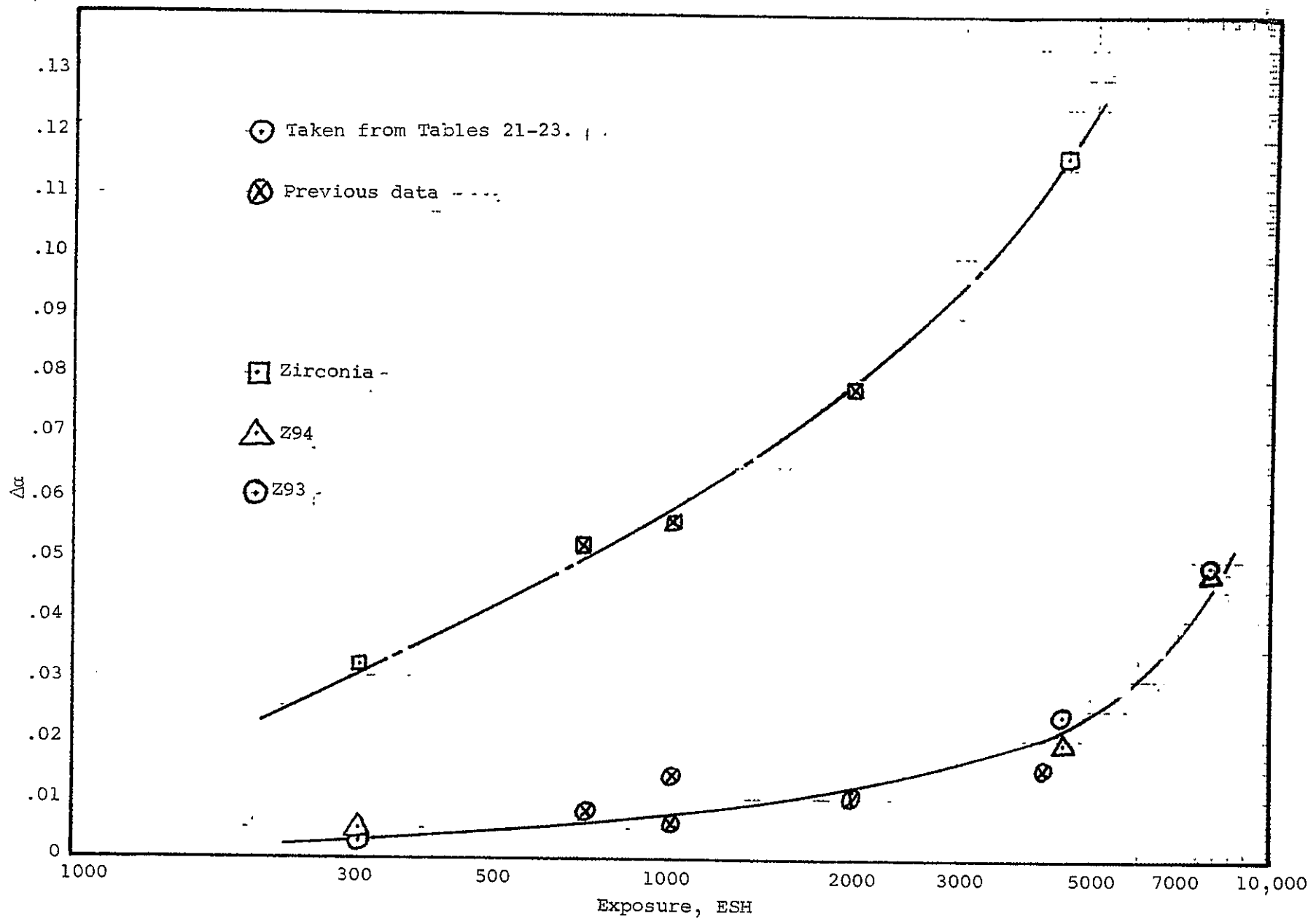
Figure 6

INCREASE IN SOLAR ABSORPTANCE OF SILICATE PAINTS AS A FUNCTION OF EXPOSURE

The stability of the S-13 coatings is a considerable improvement over earlier S-13 specimens. This is consistent with results obtained in other recent tests (ref. 4,5) and is attributed to the procedure employed in preparing the specimens. The specimens are thoroughly cured before their insertion into the vacuum chambers, and they are then thermally evacuated before irradiation.

The most stable coating in these tests was again the S-33 specimens. However, specimen 5096 (coating S-34), which in reality is an S-13 coating prepared with calcined SP500 at increased PVC (40%) and n-butanol, exhibited excellent stability with a $\Delta\alpha$ of 0.017 after 7900 ESH. The effect of catalyst concentration is indicated in Table 22 (specimens 5108 and 5106), in which the specimen employing about twice the catalyst exhibited more than twice the degradation, as shown by $\Delta\alpha$.

Little difference in effect of treatment of the Z93 specimens was noted. The Z94 specimen prepared at a PBR of 6.45 (compared to 4.3 for Z93) exhibited little improvement in stability over the Z93 specimens. The $\Delta\alpha$'s exhibited by the zirconia specimens in these tests are consistent with previous results. The increased instability of the inorganic specimens at 7900 ESH is attributed to potassium silicate degradation.

Composite degradation data are plotted in Figures 5 and 6, in which previous data for comparable intensities and preparation conditions and data obtained in tests Q-10 through Q-12 are plotted.

IIT RESEARCH INSTITUTE

58   IITRI-C6027-16

VI. ZINC OXIDE PHOTOLYSIS

A. Introduction

Zinc oxide exhibits many interesting photoproperties, particularly in its grossly impure and nonstoichiometric forms When used as a pigment in white thermal-control coatings, it brings two major advantages to the coatings: vehicle protection and unusual stability. The first of these derives from the fact that zinc oxide absorbs ultraviolet radiation preferentially and very strongly; few materials exhibit comparable absorption coefficients ($\sim 10^5$ cm^{-1}). The second advantage, however, derives from properties either unknown or poorly understood. Zinc oxide, and especially New Jersey Zinc's SP500, is practically unaffected by intense ultraviolet radiation. In an effort to elucidate the fundamental reasons for this stability, IITRI's approach has covered several areas of the problem: analyses of spectral reflectance degradation, dye photolysis, filtered radiation experiments, and literature reviews. All have served to increase our understanding of the problem and to point to more significant and productive experiments. Since previous reports (ref. 1,6) have discussed most of this work, the present discussion is confined to descriptions of our most recent work.

B. Technical Background

1. Literature Search

Since the Semiannual Report we have been studying the published literature on zinc oxide. The literature search furnished

IIT RESEARCH INSTITUTE

by JPL (ref. 8) provided nearly all of the abstracts surveyed. The great bulk of the latter document made it impossible to examine each original article. For this reason, we categorized each abstract according to whether it was very important, pertinent, interesting, or irrelevant. The bulk of the abstracts fell into the two middle categories. The basis of the classification was the relevance of the information contained to zinc oxide photolysis. In general, the information sought included:

1. Ultraviolet-radiation-induced defect formation

2. Rate and spectral nature of induced photo-responses

3. Solid state characterization of intrinsic and induced defects

4. Surface chemistry and physical processes

5. Fundamental solid state properties

6. Related photosensitive properties.

2. Basic Zinc Oxide Properties

It may be beneficial to note some properties of zinc oxide that are usually reported and agreed upon. The common observations are: (1) it is an n-type semiconductor (ref. 9-11); (2) it crystallizes in a hexagonal, wurtzite configuration (ref. 9,10); (3) it has a band gap of about 3.2 ev, which is manifest in spectral absorption (via transmittance or reflectance) measurements by an extremely sharp absorption edge at 3850 A; and (4) its photoproperties depend greatly on its purity, stoichiometry, and prior treatment. Zinc oxide is called a

semiconductor because the electron concentration in the con-
duction band is very temperature dependent. It is n-type
because the current carriers are negative (electrons). Except
for the reference to the semiconductor description, there have
been no serious objections to any of the above statements. A
few more common but less important observations might be added
to those above, including physical and optical properties, but
these will be mentioned only as necessary.

3. Absorption Scheme

Briefly, the fundamental zinc oxide absorption scheme is
as follows. First, note that all wavelengths shorter than
3850 A are absorbed fundamentally in intrinsic zinc oxide and
also that only this shorter-wavelength radiation can cause
photolytic damage. Thus wavelengths longer than the band gap
(equivalent) wavelengths are not absorbed fundamentally. The
fundamental absorption act is the release (ionization) of an
electron from the valence band to the conduction band; the
electron comes from the anion (oxygen). Though not completely
free, a conduction-band electron is not associated with any
specific atom in the crystal; hence it becomes free to wander
about the crystal. The orbital left vacant in the photoioniza-
tion process is termed a hole. Thus the process of fundamental
electronic absorption in the optical spectrum corresponds to
the creation of a hole in the valence band and an electron in
the conduction band. Since the conduction-band electron is in
a higher energy state, it will seek a lower energy state. The

IIT RESEARCH INSTITUTE

IITRI-C6027-16

possible lower energy sites can be quite numerous. The forma-
tion of an observable optical defect consequently depends upon
energy level differences, the nature and concentration of the
capturing centers, and the incident energy rate (rate of
creation of defects).

4. General Energy Level Considerations

Let us examine the following tentative scheme. A funda-
mental photon (E > 3.2 ev) is absorbed; consequently an
electron enters the conduction band, leaving a hole in the
valence band. The electron eventually reverts to a lower energy
level. If it returns ultimately to the valence band, no net
structural (or other) change has occurred. On the other hand,
if it does not revert to a lower energy level, at least two new
structures (defects) result: a hole and an electron captured
at a defect site. Figure 5 shows that the number of possible
transitions increases greatly with the number of energy levels,
E_i, and the number of trapping centers in each, N_i. In general,
two types of trapping centers (traps) can be distinguished.
The first trap is destroyed (annihilated) in the absorption
act (e.g., an F center capturing an electron becomes an F'
center in the process, creating one more F' center and one less
F center). The second type of defect absorbs radiation by
being excited rather than ionized. The excitation can be dis-
sipated in a number of ways. The net effect of an excitation
process is to expend energy without changing the basic identity
of the absorbing center.

The above discussion will serve as a basis for understanding or interpreting the many photoreactions that zinc oxide can undergo. The primary ultraviolet absorption act in zinc oxide corresponds to the reaction:

$$ZnO \xrightarrow{h\nu_f} ZnO^+ + e_c^- \qquad (1)$$
$$ZnO^*$$
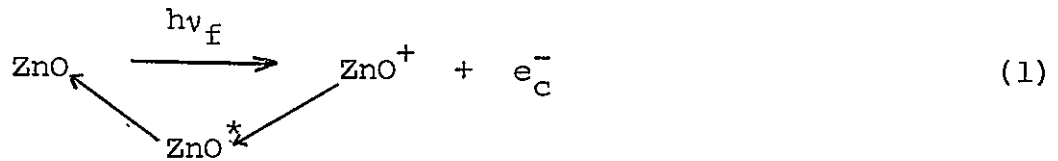
where e_c^- denotes an electron in the conduction band. The notation ZnO^+ signifies a hole, and ZnO^*, an excited (exciton) state. The conduction band is labelled C, and the valence band is designated by V. The primary absorption act has been labelled 1 in Figure 7.
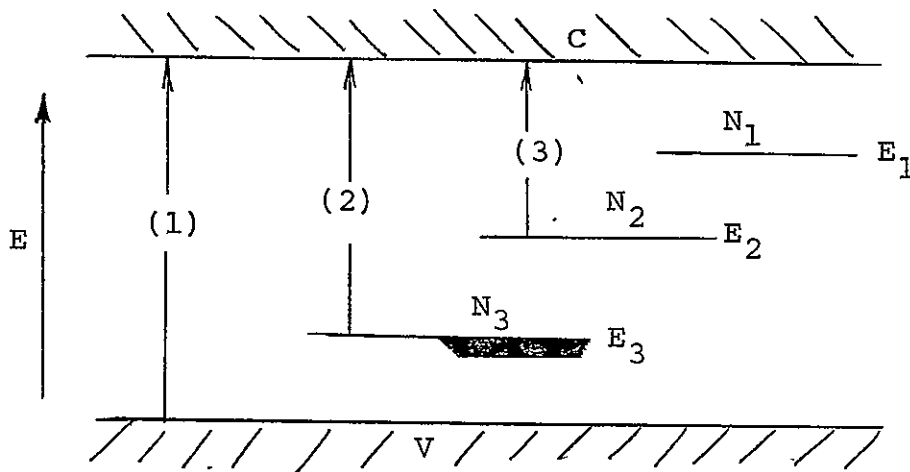
Figure 7

GENERALIZED BAND SCHEME OF DEFECTS IN FORBIDDEN ZONE

Of major interest is the fate of the conduction-band electron when it does not return to the valence band. As shown in Figure 7, this electron can drop to one of several levels

Depending upon the individual nature of these levels after the trapping of the electron, they may absorb longer wavelength radiations in such transitions, termed interband, as in the transitions E_2 to E_1, E_1 to C, and E_2 to C. Other transitions might be E_1 to E_1^*, etc., which would be termed intraband transitions and would correspond to infrared absorption. This allows further absorption possibilities such as E_2^* to E, and E_2^* to E_1^*, etc.

5. The Zinc Oxide Photolysis Problem

Experimental data support the supposition of at least two distinct levels that cause zinc oxide to absorb at visible wavelengths. Figure 8 shows an energy level diagram constructed on the basis of two such levels, 0.40 ev and 0.80 ev above the valence band. Determination of the nature of the defects, D_1 and D_2, is precisely the primary objective of the photolysis studies. Once identified, the mechanisms and kinetics of their formation and annihilation can be more readily studied.
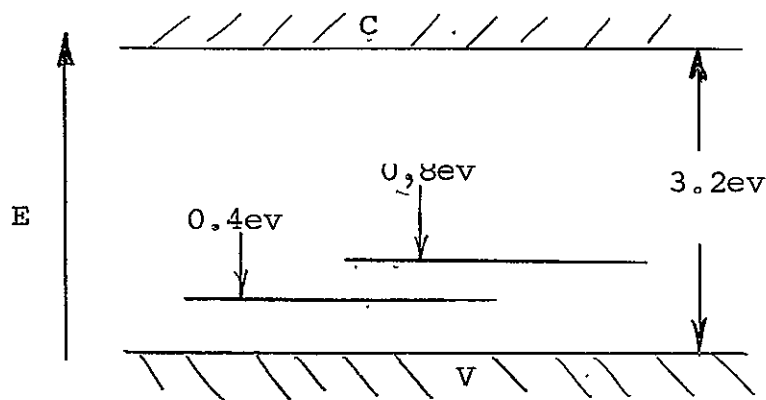
Figure 8

POSSIBLE BAND SCHEME OF ZINC OXIDE DEFECTS

IITRI-C6027-16

C. Literature Search

1. Research Results

After reviewing the conclusions of several other experimenters and after their own experimental work, Zelikin and Zhukovskii (ref. 12) conclude that the presence of oxygen is essential to the formation of yellow luminescence centers and further that an excess of oxygen and some kind of structural defect are necessary to the development of yellow luminescence. On the other hand, they remark that the green luminescence band is observed only when oxygen difficiencies exist in the lattice. In both cases, they claim that the bands are inherent properties; their magnitudes can be enhanced or suppressed by impurities but do not depend qualitatively upon their presence or absence.

The above conclusion regarding the green luminescence accords with that of Heiland et al (ref. 10), who associate it with a stoichiometric excess of zinc, which, as they suggest, serves as the activator. Likewise, these authors seem to agree that the yellow luminescence center is a zinc deficiency.

In their article on zinc oxide photoconduction, Collins and Thomas (ref. 13) conclusively establish the effect of oxygen pressure on photoconduction. They propose that holes from hole-electron pairs discharge lattice-oxygen ions at the surface, producing a surface excess of zinc and an electron-enrichment layer in which conduction occurs. They have also measured the quantum efficiency of the ultraviolet absorption process,

i.e., the number of conduction electrons formed per incident UV photon. The quantum efficiency starts at about 0.25 and drops several orders after exposure to $\sim 10^{16}$ photons/cm^2 ($\lambda \leq 3650$ A). Interestingly enough, their work also demonstrates reciprocity in photoconductance and indicates that the spectral quantum efficiency curve follows the fundamental optical absorption edge very closely. Collins and Thomas (ref. 13) propose that the holes from the hole-electron pairs produced by the UV-absorption act diffuse to the surface and become trapped on oxygen ions, discharging them to form free oxygen. The ability to follow this process through measurements of surface conductivity gives a measure of the rate of creation of defects.

Heiland (ref. 14), Medved (ref. 15), Melnick (ref. 16), Barry and Stone (ref. 17), Gerritsen et al (ref. 18), and Thomas and Lander (ref. 19) confirm that the UV-induced changes in zinc oxide are essentially surface effects and that they are clearly related to photo-induced oxygen desorption. Heiland (ref. 14) finds a rate dependence (1/3 to 1/2 power) of photo-conductivity on irradiation intensity. Collins and Thomas (ref. 13) found reciprocity between quantum yield and radiation intensity for very nearly the same irradiation rates and conditions as Heiland's; the explanation may have to do with different trap densities and free-carrier lifetimes. Heiland also suggests that the observed photoconductivity occurs in the conduction band and is augmented by conduction in an impurity band electron trap slightly below the conduction band.

Medved (ref. 15) corroborated Melnick's theory (ref. 16) by correlating photoconductivity with oxygen desorption; Cimino et al (ref. 20) obtained the same effect and reached conclusions similar to those of Medved and Melnick. Barry and Stone (ref. 17) definitely confirm these findings and go on to discuss a model viewing zinc oxide as an n-type semiconductor with interstitial zinc and with oxygen chemisorbed as O^- and O^{--}. Although they consider that interstitial zinc plays an important mechanistic role, they do not suggest it is an electron donor, as do Heiland and Thomas and Lander.

The experiments of Gerrsitsen et al (ref. 18) also demonstrated that the free carriers in zinc oxide are electrons; hole motion was not found. Also, they calculated a trap density of $10^{14}/cm^3$ for the position of the Fermi level 0.8 ev below the conduction band and of $10^{17}/cm^3$ for its position 0.4 ev below the conduction band. The latter values suggest a distortion of the energy levels of the interstitial zinc with increasing defect concentration. Zelikin and Zhukovskii (ref. 12) also briefly discussed this possibility but dismiss it for lack of supporting evidence. Miller (ref. 21) reviews the work of Medved and others and extends Medved's theory of chemisorption and conductivity.

Mollwo (ref. 22) summarized much of what had been known about zinc oxide up to 1954. Among other remarks, Mollwo states the following:

(a) The dark conductivity of ZnO is due to an excess of interstitial zinc.

(b) The interstitial zinc dissociates thermally according to the equation:

$$ZnO \xrightleftharpoons{\text{therm}} Zn^{+}$$
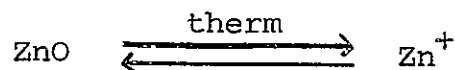
(c) Irradiation removes a second electron (in a very thin surface layer) due to very strong UV absorption.

$$Zn^{+} \xrightleftharpoons{\text{opt}} Zn^{++}$$
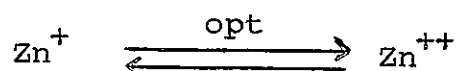
(d) In fundamental absorption, an electron is removed from the valence band to the conduction band, leaving a hole in the valence band. In intrinsic zinc oxide the electron and hole recombine so rapidly that photocurrents are not observed. But if Zn^{+} ions are present, the holes can also disappear by combining with Zn^{+} ions, forming Zn^{++} ions.

(e) Recombination of electrons (in the conduction band) with Zn^{++} is much slower than that of electrons and holes.

(f) Quantum efficiencies will be proportional to Zn^{+} concentration.

(g) A slow, irreversible photoelectric process, much less understood, apparently arises from the combination of oxygen ions and holes to give atomic oxygen, which then desorbs. Also, this must be a surface effect because oxygen diffusion is negligible in zinc oxide at room temperature.

(h) In zinc oxide crystals containing a stoichiometric excess of zinc, a yellow absorption band developed. A correspondence between the number of conduction electrons, estimated from conductivity data, and the concentration of absorption centers was found. (The latter value was obtained from Smakula's formula for absorption bands. This correlation strongly supports the singly ionized, interstitial zinc assignment to this band, but Mollwo does not give further details, such as the

IIT RESEARCH INSTITUTE

center frequency, oscillator strength, or width of the band that he analyzed to obtain this correlation.)

In addition to studies in the fundamental and optical spectra of zinc oxide, there have been a large number of studies made in the infrared. Matsushita and Nakata (ref. 23) studied a band at 1550 cm^{-1} (6.45 μ) and, from a correlation of free electrons with band shape and intensity, attributed it to Zn vacancies with trapped electrons.

Thomas (ref. 24) also noticed that strong absorption can arise from the presence of free electrons. Thomas measured the free electron concentrations and correlated these with intrinsic absorption in the 1- to 12-μ wavelength region. He reports that the absorption coefficient, α, varies approximately as λ^3 for $\lambda < 5$ μ and is less steep for $\lambda > 6$ μ; at any given λ, α varies directly as the free electron concentration. Finally, Thomas examines and concludes that, although further theoretical work is necessary to make a detailed accounting of his data, a rough agreement between theory and experiment is found.

Filiminov (ref. 25) observed that infrared absorption increased after removal of surface-absorbed oxygen. The oxygen was removed by UV irradiation in vacuo. The author assumes that the desorption of oxygen is accompanied by an increase in the concentration of conduction electrons due to release of electrons formerly bound to the adsorbed oxygen. Hence, the appearance of an infrared absorption band is, in his view, naturally associated with an increase in the number of conduction

electrons. Absorption then would be caused by electron transi-
tions from donor levels to the conduction band or by transitions
within this band. He observes that the depth of local levels
caused by excess zinc varies over a wide range (0.6 to 0.1 ev)
with the concentration of excess zinc. The variable trap depth,
as Filiminov points out, makes it difficult to predict the
frequency of maximum absorption. From his data, however, he
concludes that the monotonic increase in absorption with increas-
ing wavelength suggests an intraband transition.

In an experiment somewhat similar to the above, Miloslavskii
and Kovalenko (ref. 26) studied the electrical and optical prop-
erties of thin, sputtered films of zinc oxide. Through observa-
tions of properties versus film thickness, they were able to see
a strong surface effect. In attempting to correlate absorption
with electrical conductivity through the Drude relationship
they obtained poor agreement at short wavelengths (1 to 4 μ);
the presence of a clearly expressed maximum at 5.5 μ, which they
attributed to quantum transitions, produced a marked discrepancy
in the correlation. They, too, have shown a direct proportion-
ality between long-wavelength absorption and electrical
conductivity and, as Filimonov does, associate it with conduc-
tion-band electrons.

A study of the relationships between spectral reflectance
(1 to 45 μ) and free carrier concentration by Collins and
Kleinman (ref. 27) resulted in what they describe as an excellent
fit to the data. They found that in samples with free carrier

concentrations below 10^{16} cm^{-3}, the usual reflectance spectrum of an ionic crystal is observed but that the contribution to the optical constants becomes significant for concentrations in excess of 10^{17} cm^{-3} They claim a good fit over the range 1 to 45 μ. This of course contrasts with the previous author's results, but it may be that the very high carrier concentration ($\sim 10^{20}$ cm^{-3}) used in the work of Miloslavskii and Kovalenko was not considered in Collins and Kleinman's effort.

2. Summary

Evidently, most of the difficulties in the reproducibility of experimental results can be attributed to sample preparation and treatment. Reproducibility can be readily demonstrated in most experiments when the same crystal is used, but it is quite unusual from one sample to the next, particularly when the samples have been prepared in different laboratories. Nevertheless, it appears that the normal state of undoped zinc oxide must contain singly ionized (thermally) zinc ions. Zinc oxide stoichiometry varies widely among samples, but inevitably it favors an excess zinc or oxygen-deficient structure. Other questions provoked by the article referenced and discussed are concerned with (a) whether Zn^+ is substitutional, interstitial, or otherwise, particularly when its optical ionization energy is given as 3.2 ev; (b) the thermal activation energy of the $Zn \rightarrow Zn^+$ transition; and (c) the energy levels associated with singly and doubly charged oxygen ions in the zinc oxide crystal lattice.

One purpose of the study was to learn more about the basic solid state behavior of zinc oxide in the hope that a connection could be made between optical and other surface properties of zinc oxide. Numerous studies have been made to relate various responses, e.g., photoconductivity and photodesorption, catalysis and adsorption, and electrical conductivity and infrared absorption. Unfortunately, a systematic study of any of these with visible reflectance has not been made. Although it is obvious that there are other useful relationships, e.g., between luminescence and visible reflectance, it is not so obvious what they are. In general, the latter statement seems to be applicable to the whole zinc oxide photolysis problem.

D. Analysis

1. Possible Defects

The majority of primary events following UV absorption are direct combinations via exciton transitions, but electrons in the conduction band may nevertheless be trapped by several possible trapping centers, e.g., physically adsorbed oxygen, singly or doubly ionized zinc ions, oxygen vacancies, or impurities. In vacuum, however, the physically adsorbed oxygen concentration should be extremely small initially and thus should have a relatively negligible effect. This assertion removes the Melnick model from further serious consideration. Doubly ionized zinc ions would be very effective traps and would be highly mobile. Oxygen vacancies and chemisorbed oxygen offer additional

possibilities in trapping sites. Impurities, of course, may provide even more electron-capture cross sections.

2. Tentative Photolysis Scheme

By ruling out impurities, Zn^+, Zn^{++}, and oxygen vacancy defect structures remain. Therefore, based on our observations, on the conclusions expressed in the literature, and on a series of definitive experiments, we can construct a tentative scheme for zinc oxide photolysis. Analyses have been made of ΔR_λ curves taken from UV-irradiated zinc oxide paints (both silicate and silicone vehicles) under normal conditions, at high temperatures, and with different spectral radiant intensities. The identical ΔR_λ curve shapes, independent of irradiation circumstances, stand out as a very important feature of zinc oxide photolysis. Bleaching or thermal annealing, if they do occur at all, must be negligible. The spectrum obtained in nearly every case is typified by the differential absorption spectrum shown in Figure 9.

Because of their relevance here, we relate the main findings of a recent study to the determination of the effects of a modified AH-6 spectrum containing essentially no visible or near-infrared radiation versus those of an AH-6 spectrum modified only to the extent of cutting off radiation with $\lambda < 2200$ A. The resultant ΔR_λ spectra showed no qualitative differences, but the magnitudes could be related to total ultraviolet dose ($\lambda < 3850$ A). An earlier test in which zinc oxide-silicate samples were exposed to ultraviolet at temperatures of 400, 500,

and 600°F indicated that the ΔR_λ curves for samples exposed to ultraviolet and high temperature and to temperature only, though quantitatively different, were qualitatively identical and that each could be represented by the spectrum in Figure 9.
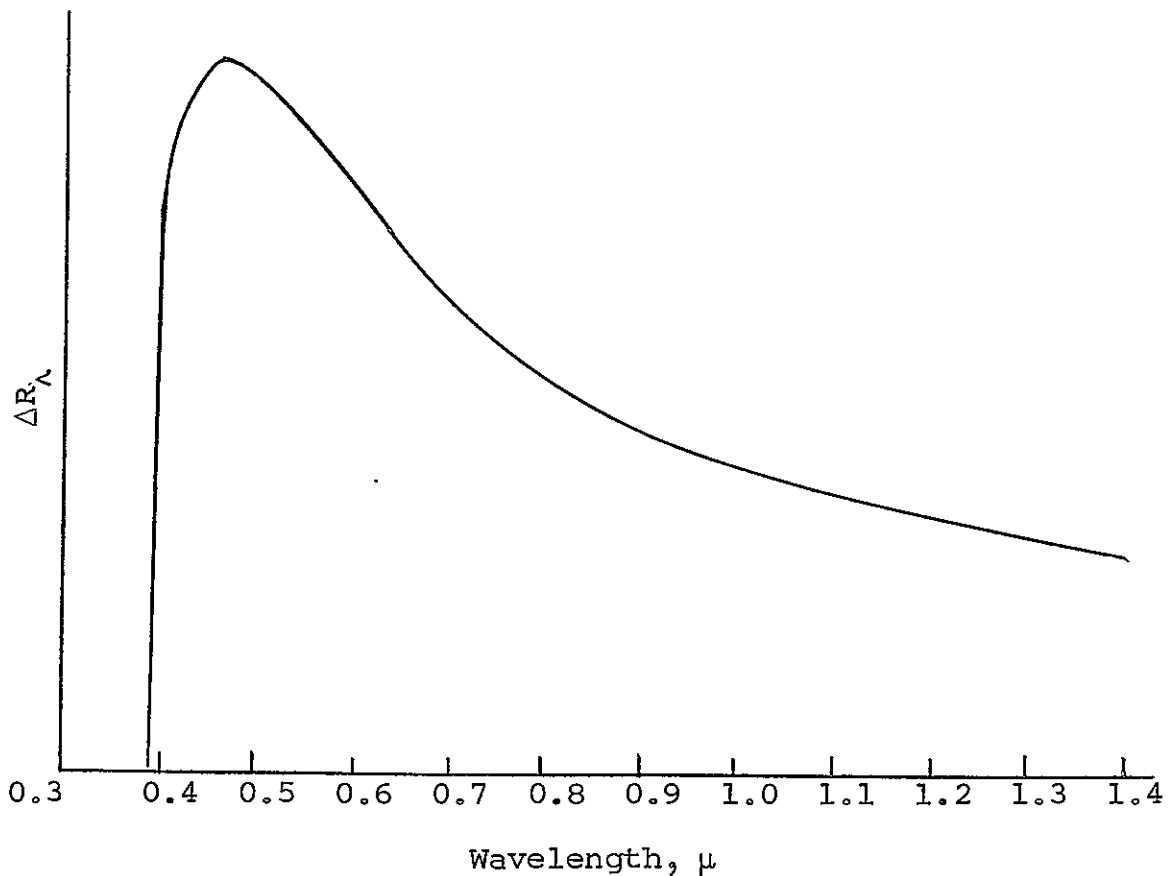
Figure 9

TYPICAL ZINC OXIDE-INDUCED ABSORPTION SPECTRUM

These results are consistent with the bleaching experiment reported previously (ref. 28) in which defect annealing or bleaching in an irradiated zinc oxide paint, even with the

IIT RESEARCH INSTITUTE

IITRI-C6027-16

admission of oxygen, could not be detected either immediately after or up to more than 6 hr after cessation of irradiation. Such behavior weighs heavily against Melnick's model.

Zinc oxide spectral reflectance degradation must be associated with defects that are neither thermally deactivated nor very sensitive to changes in partial pressure of oxygen. This excludes Zn^+ in any simple configuration; such an exclusion is supported by the evidence that the optical ionization energy for the reaction $Zn^+ \rightarrow Zn^{++}$ is 3.2 ev (ref. 22). Hence the resulting optical absorption, coinciding with the fundamental absorption, would not significantly affect visible reflectance. In fact, a band at 3.2 ev has been found, not after ultraviolet irradiation, but after mechanical treatment.

The shape of the spectrum in Figure 9 suggests at least two responsible defects, but it is very difficult to identify precisely the number and nature of each. Nevertheless, it appears that the ratio of the concentration of these defects remains nearly constant.

The model proposed by Melnick (ref. 16) represents only a minute part of the true model but can be used as a starting point in the understanding of the photolytic scheme. The exclusion of Zn^+ as a major optical defect, however, does not necessarily remove it from the model. In any event, the Collins-Thomas model can be adopted with certain amendments. Thomas (ref. 24), Heiland (ref. 14), and Zelikin and Zhukovskii (ref. 12) have all produced evidence to the effect that the hypothesis of a

JIT RESEARCH INSTITUTE

75

structural defect must be invoked in order to explain certain of the electrical and optical phenomena displayed by zinc oxide under ultraviolet irradiation.

3. Defect Schemes

A tentative construction of the photolytic degradation scheme can be developed in the following way. We described the chemistry of the basic ultraviolet absorption act as:
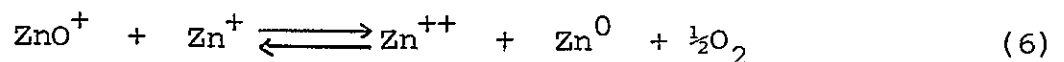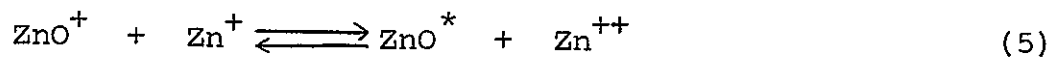
$$ZnO + h\nu_f \longrightarrow ZnO^+ + e_c^- \qquad (1)$$
$$\searrow ZnO^* \nearrow$$
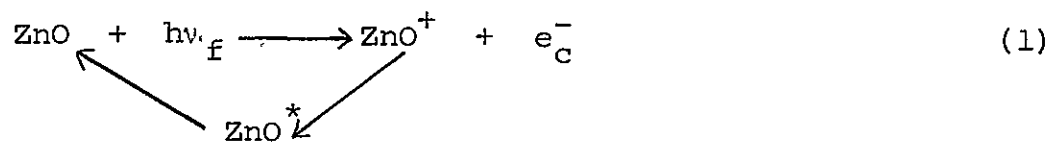
The hole from the electron-hole pair, except in recombination, reacts preferentially with chemisorbed oxygen (O^-), giving (in Melnick's model):

$$ZnO^+ + O^- \rightleftharpoons ZnO^* + \tfrac{1}{2}O_2 \qquad (2)$$
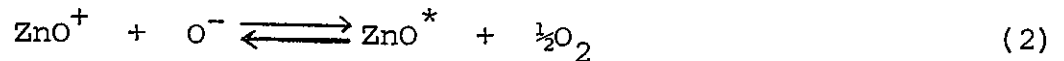
The oxygen thermally desorbs almost immediately. The net result (so far) is the addition of an electron to the conduction band and the loss of one oxygen atom from a chemisorption surface site. The Collins-Thomas model gives:

$$ZnO^+ + O^{--} \rightleftharpoons ZnO^* + O^- \qquad (3)$$
$$ZnO^+ + O^- = ZnO^* + \tfrac{1}{2}O_2 \qquad (4)$$
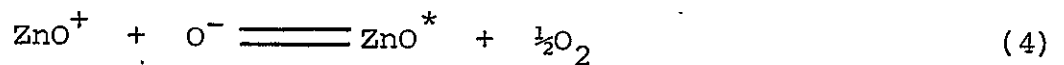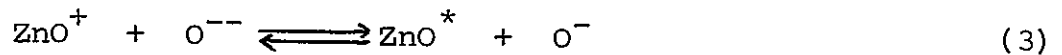
In addition to the above reactions, the following are also important:

$$ZnO^+ + Zn^+ \rightleftharpoons ZnO^* + Zn^{++} \qquad (5)$$
$$ZnO^+ + Zn^+ \rightleftharpoons Zn^{++} + Zn^0 + \tfrac{1}{2}O_2 \qquad (6)$$

$$O^- \xrightarrow{h\nu_1} \tfrac{1}{2}O_2 \ + \ e_c^- \quad \text{(direct ionization)} \qquad (7)$$

$$Zn^+ \ + \ h\nu_f \rightleftharpoons Zn^{++} \ + \ e_c^- \qquad (8)$$

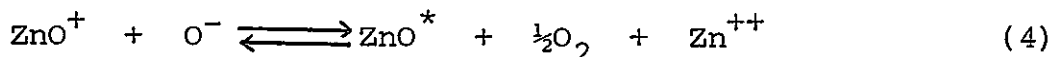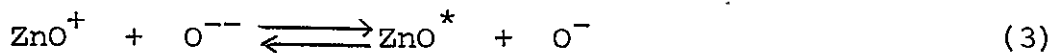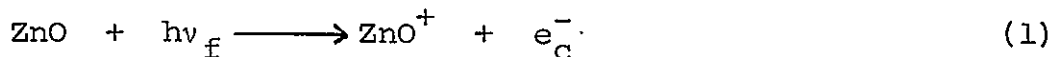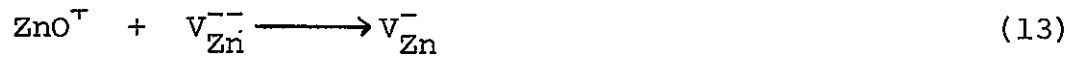$$Zn^+ \ + \ O^- \rightleftharpoons ZnO^* \qquad (9)$$
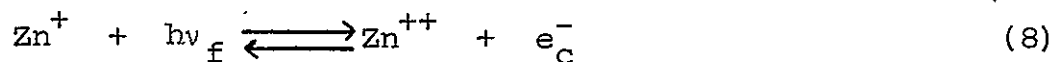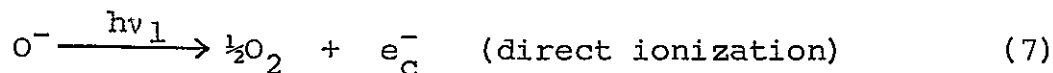
Other reactions undoubtedly could be written, but our intent here is to write only those that are important to the models. The Collins-Thomas model (Equations 3 and 4) for oxygen desorption will lead to an intensity rate dependence with an exponent of 0.5. The photoconductivity data of Collins and Thomas (ref. 13), though showing reciprocity, consistently exhibit only very small rate effects. (A crude analysis of their data gives the rate dependence of photoconductivity as $I^{1.1}$, which would not importantly affect reciprocity).

4. Tentative Model

After careful consideration we would choose the following reactions as those directly responsible for optically important photolysis:

$$ZnO \ + \ h\nu_f \longrightarrow ZnO^+ \ + \ e_c^- \qquad (1)$$

$$ZnO^+ \ + \ O^{--} \rightleftharpoons ZnO^* \ + \ O^- \qquad (3)$$

$$ZnO^+ \ + \ O^- \rightleftharpoons ZnO^* \ + \ \tfrac{1}{2}O_2 \ + \ Zn^{++} \qquad (4)$$

$$V_0^{++} \ + \ e_c^- \longrightarrow V_0^+ \qquad (10)$$

$$Zn^0 \xrightarrow{therm} Zn^+ \ + \ e_c^- \qquad (11)$$

$$Zn^+ \ + \ h\nu_f \longrightarrow Zn^{++} \text{ (interstitial) } + \ V_{Zn}^{--} \qquad 12)$$

IIT RESEARCH INSTITUTE

$$\text{ZnO}^\top \;+\; V_{Zn}^{--} \longrightarrow V_{Zn}^- \qquad\qquad (13)$$
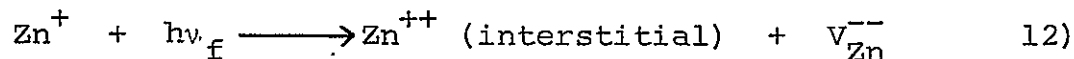
The induced absorption (negative differential reflectance) is due to the reactions:

$$V_0^+ \;+\; h\nu_g \longrightarrow V_0^{++} \;+\; e^* \qquad\qquad (14)$$

and

$$V_{Zn}^- \;+\; \qquad \longrightarrow V_{Zn}^0 \qquad\qquad (15)$$
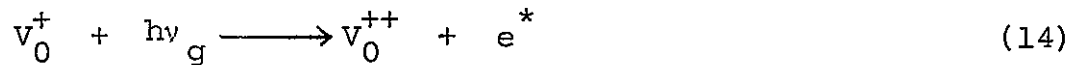
where V signifies a vacancy; its subscript identifies the type of vacancy, and its superscript the effective change at the vacancy site. Equations 10 and 13 denote an electron captured by an oxygen vacancy and a hole trapped by a zinc vacancy, respectively. The inverse reactions (Equations 14 and 15) represent the absorptions responsible for UV photolysis of zinc oxide. These assignments can be shown to possess the properties discussed earlier.

A negative surface charge builds up due to the free electrons, but charge neutrality is preserved by an equal and opposite (positive) charge buildup due to the highly mobile Zn^{++}. The negative charge buildup decreases the photolytic process by limiting the effective electron diffusion rate to the surface, making an increasingly greater fraction of electrons available for radiationless recombinations with holes.

6. Summary

The above model, as it stands, should be regarded as tentative. Many aspects of this model remain to be verified. Certainly, an important factor missing from the model is kinetics;

IIT RESEARCH INSTITUTE

IITRI-C6027-16

another is a theoretical verification of these assignments. All in all, though, it appears that these assignments accord very well with the observed behavior of UV-irradiated zinc oxide materials and hence must be given serious consideration.

VII. SPECIFIC PROBLEM AREAS

A. Contamination

Anomalous degradation has been observed in a number of white coatings of all types. These instances have always been random and nonselective within the test chamber in which they occurred. For example, anomalous degradation was observed in an S-13 paint specimen that was applied directly to the refrigerated sample table (-38°F) in an early test. This degradation was attributed to the accumulation of volatile contaminants (from warmer, adjacent S-13 specimens), which condensed on the surface of the colder samples. The contamination was thought to result from unreacted amine catalyst present in the S-13 coating, which may have been placed in the space chamber too soon after preparation.

Other instances of anomalous degradation that have occurred are explicable only in terms of coating contamination before insertion into the simulation chambers. Steps are therefore taken to ensure that all coatings are fully cured before exposure.

A general trend toward greater stability in the S-13 and S-33 coatings has been observed since thermal evacuation procedures have been instigated before irradiation. This procedure involves soaking the specimens for 16 hr at about 180°F in vacuum before exposure to ultraviolet. This is accomplished by epoxying the specimens to the sample table and passing hot tap water through the table. The samples are then cooled with cold

IIT RESEARCH INSTITUTE

80   IITRI-C6027-16

tap water (45°F) during the simulation test, unless a specifically different temperature is desired.

B. Lattice Distortion of Zinc Oxide

Yellowing of zinc oxide powders as a result of mechanical distortion was first noted in Report No. IITRI-C207-25. Yellowing can be produced by scratching the surface of a zinc oxide-silicate coating, grinding the powder with an agate mortar and pestle, and compacting the powder at high pressures. It has since been found that the very process of paint manufacture that involves grinding the pigment into a vehicle (in order to wet the particles) will cause mill yellowing if shear forces are excessive (ref. 3). Excessive shear forces can result from operation at too high a ratio of grinding media (porcelain balls) to mill charge or if the mill is operated at too high a speed. The effect of grinding time is therefore important, and studies concerning this problem are documented in reference 3.

The effect of mechanically yellowing SP500 zinc oxide on the stability of an S-13 coating prepared from the yellow pigment was recently studied (ref. 4). This was accomplished by carefully grinding the pigment in an agate mortar and pestle and by using it in LTV-602. The solar absorptance increase was 0.049 in a 2000-ESH expsoure, which compares quite unfavorably with a standard S-13 irradiated in the same test ($\Delta\alpha$ = 0.027).

C. Specimen-Handling Procedures

In general, the main advantages of post-exposure reflectance measurements are simplicity, expediency, sample volume,

and, except for the problem posed by oxygen bleaching (which is accelerated by exposure to light), more accuracy. Indeed, when there is the possibility of oxygen bleaching, both sample-handling techniques and reflectance-measurement techniques become more critical.

For integrating-sphere spectral reflectometers, which employ polychromatic, undispersed, incident light, it is necessary that the measurements begin with the lower wavelengths, i.e., the near ultraviolet. Thus, bleaching (which usually occurs near the lower wavelength absorption edge) is minimized during the measurements when this wavelength interval is measured first. Integrating-sphere spectroreflectometers, which employ monochromatic, dispersed, incident light, greatly reduce this problem.

When post-exposure measurements are necessary and particularly when the possibility of bleaching is prevalent, it is necessary to minimize atmospheric involvement by maintaining the specimens in the dark and in vacuum. In the event that evacuation is impractical, then the specimens must be maintained under a positive pressure of a dry, inert atmosphere. It should be noted that bleaching by diffusion of oxygen into the system has been observed as being a function of temperature. It has also been observed to occur in the dark, although more slowly. Thus, the possibility of reaction with oxygen can be further reduced by maintaining samples at low temperatures after exposure.

VIII. SUMMARY

The most significant results obtained during the program are as follows.

1. The bleaching, or reflectance increase, in the infrared region(α_2) exhibited by silicate paints is attributed to loss of water on irradiation. Similarly, the loss in infrared reflectance when heat-treated specimens are allowed to age is attributed to the reabsorption of water. However, a 800°C heat treatment appears to minimize the reabsorption of water.

2. The stability of zinc oxide-pigmented potassium silicate paints is not affected by the relative humidity during application and cure. However, superior adhesion is exhibited by specimens cured at 0% RH.

3. Storage in Mylar, H-Film, and Lexan films appears to provide excellent protection for potassium silicate coatings.

4. The use of SP500 zinc oxide calcined for 16 hr at 650°C improves the stability of S-13 coatings.

5. Dow Corning's Q92-002, prepared from their proprietary RTV at an SP500 concentration of 35% PVC, compared favorably with S-13 in a single 2000-ESH exposure.

6. General Electric's SR585 and Dow Corning's Silastic 280 silicone adhesives are excellent pressure-sensitive bonding agents for S-13 films and do not affect the stability of the resultant composites.

7. The experimental silicone resins developed under this and the previous JPL program (ref. 1) provide the most stable zinc oxide-pigmented coatings examined under this program.

8. The important parameters in assuring stability in silicone paints appears to be (a) completeness of cure, (b) minimization of curing agents, (c) minimization of residual solvent, especially aromatic solvents, in irradiated paints.

IIT RESEARCH INSTITUTE

9. Ultraviolet irradiation plus heat produce greater damage than either parameter alone; higher temperatures lead to greater damage, and, in general, high pigment concentrations are more stable from an optical standpoint.

10. The sensitivity of a given coating to ultraviolet intensity must be evaluated before accelerated testing can be relied upon. S-13 and Z93 are relatively insensitive to intensity between 5 and 15 solar intensities (and at most, exhibit an inverse dependence on solar factors). Zirconia-silicate paints, on the other hand, are definitely sensitive to intensity. The degree of sensitivity of all coatings is increased by lack of substrate cooling, wherein thermal effects become important.

11. Filtered-ultraviolet-radiation tests indicate that degradation depends much more sensitively on total exposure than on the spectral character of the incident radiation. Therefore, the AH-6 lamp does not present a problem relative to its high percentage of ultraviolet, and it adequately simulates the effects of extraterrestrial solar radiation in this respect. Furthermore, the high percentage of ultraviolet makes the AH-6 an ideal source for accelerated testing.

12. Long-term tests (7900 ESH) indicate that zinc oxide-methyl silicone paints exhibit little increase in solar absorptance after 3000 ESH. Zinc oxide-silicate paints, on the other hand, exhibited increased instability as a function of exposure after about 5000 ESH. The difference is attributed to degradation of potassium silicate after about 5000 ESH.

APPENDIX I

COMPUTATION OF SPACE-SIMULATION EXPOSURES

The total exposure in equivalent sun-hours of radiation (ESH) received by a specimen is calculated from a plot of solar intensity versus time. A typical plot of intensity versus time is presented in Figure 10, which is taken from test Q-8. In test Q-8, the samples receiving high-intensity radiation were located 4-5/16 in. from the lamp; the lamp-to-sample distance for the low-intensity irradiation was 8-13/16 in. Thus, the average intensity for the low-intensity irradiation was 3.9 suns, and for the high-intensity irradiation, 12.4 suns.

IIT RESEARCH INSTITUTE

IITRI-C6027-16
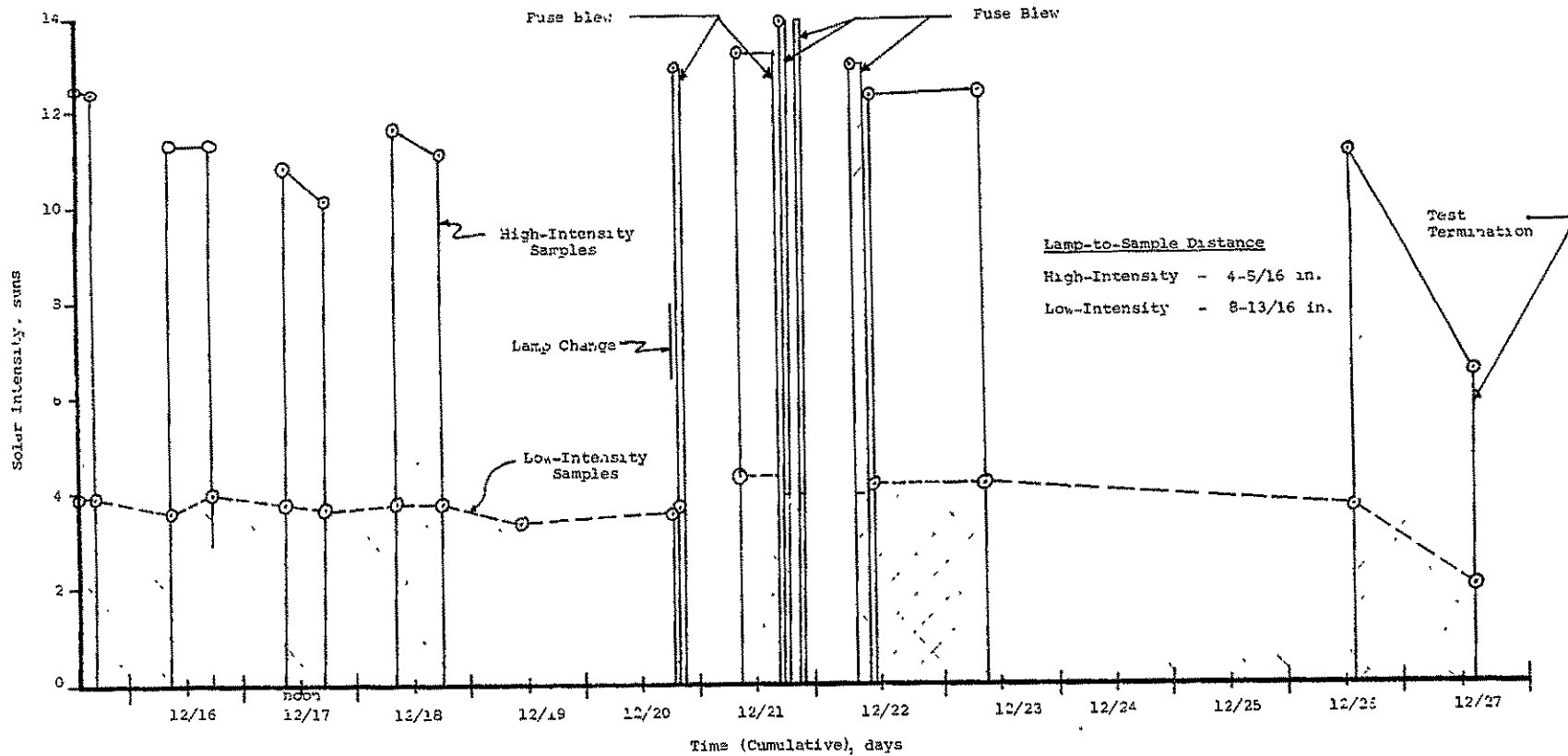
Figure 10

TEST Q-6 IRRADIATION SCHEDULE

APPENDIX II

DETERMINATION OF AH-6 LAMP OUTPUT

Data presented in this report are based upon the assumption
that one-half of the AH-6 lamp's energy lies below 4000 A. Other
data indicated that considerably less than one-half the lamp's
energy is below 4000 A. Therefore the lamp output was determined
experimentally.

The lamp output was determined by using the following
equipment: an Eppley 6074 thermopile, an Eppley type S pyrohe-
liometer, a used AH-6 lamp, a 3-7A filter, and a 7-54 filter.
Figure 11 shows the transmission of the filters and the output
of an AH-6 lamp from the General Electric data.*

An old lamp was used with the Eppley 6074 thermopile and
the two filters to determine the ratio of millivolts to total
lamp output. At least three measurements of thermopile output
were made at each of the following distances from lamp center-
line to thermopile face: 10, 12.5, 15, 20, 25, 50, and 75 cm.
The thermopile was allowed to cool between readings by closing
the steel shutter and inserting a cardboard shutter between the
thermopile and the lamp. The sensitivity of the thermopile is
rated at 0.150 mv/mw-cm^{-2}. Table 24 shows the comparative
signals with and without one of the two filters.

The fraction of ultraviolet energy below 4000 A was computed
as the average value obtained from the energy passed by the 7-54
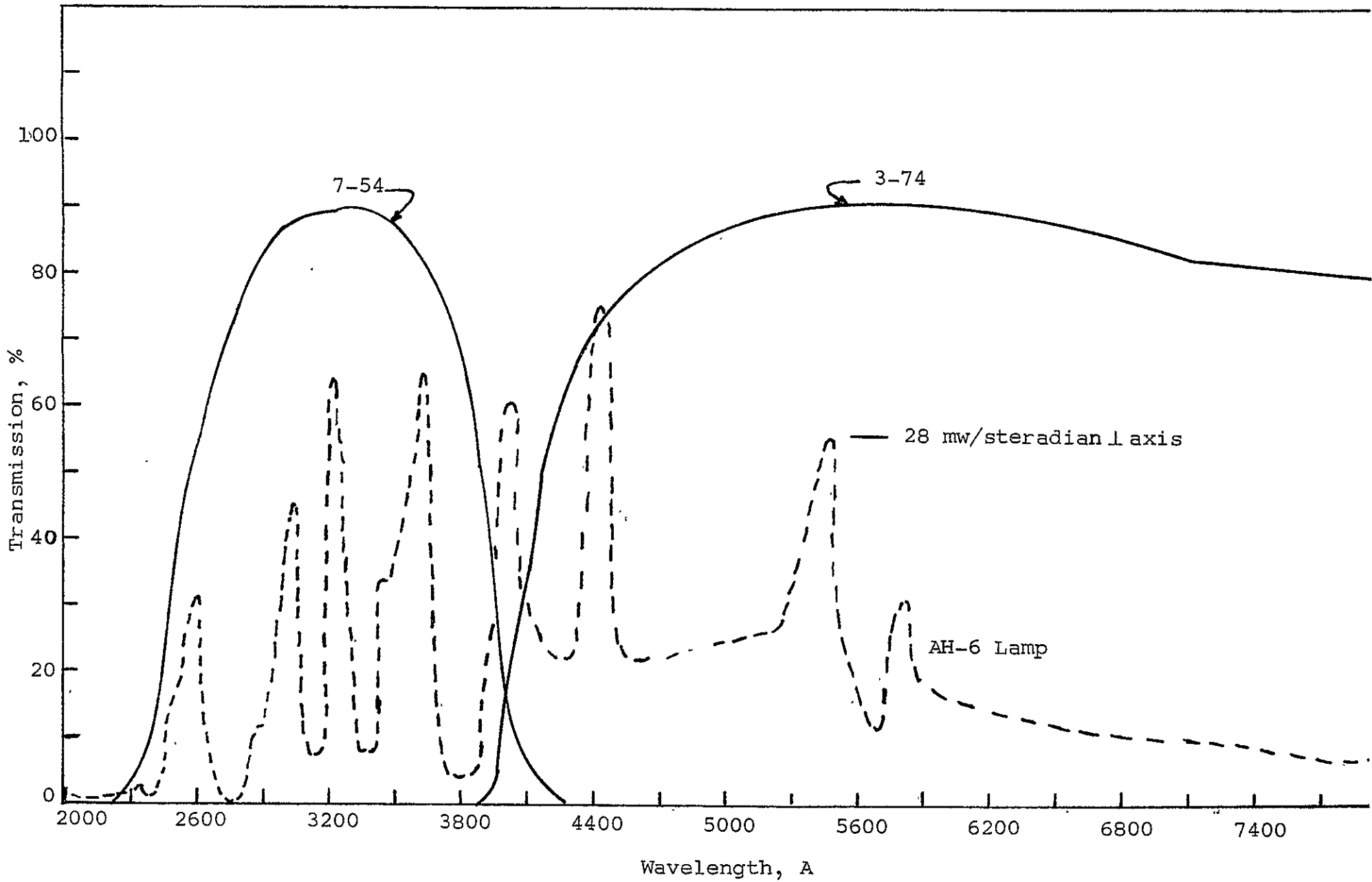
*General Electric Catalogue FN-412(10-59), p. 17.

IIT RESEARCH INSTITUTE

87

Figure 11

SPECTRA OF FILTERS USED TO DETERMINE AH-6 LAMP OUTPUT

Table 24

DETERMINATION OF UV OUTPUT OF AH-6 LAMP

| Source-to-Detector Distance | | Output, EMF | | | Ultraviolet Fraction | | |
in.	cm	TR	UV	VI	UV/TR	(UV - VI)/TR	Average Factor[a]
3.94	10	17.97	6.46	10.45	0.36	0.42	0.39
4.92	12.5	12.75	4.50	7.54	0.35	0.41	0.38
5.90	15	9.46	3.22	5.46	0.34	0.42	0.38
7.87	20	5.76	1.93	3.32	0.34	0.42	0.38
9.83	25	4.61	1.52	2.60	0.32	0.44	0.38
19.70	50	1.23	0.42	0.68	0.33	0.45	0.39
29.50	75	0.63	0.19	0.38	0.29	0.38	0.34

[a]Average factor $= \dfrac{\dfrac{UV}{TR} + \dfrac{(TR - VI)}{TR}}{2}$

Note: TR, total radiation; UV, using 7-54 filter; VI, using 3.74 filter.

89

filter (Figure 11) and the energy not passed (filtered out) by the 3-74 filter. The average value, shown in the last column in Table 24, is approximately 0.38. Thus the exposure data presented in this report should be multiplied by 0.76 (0.38/0.5) for better accuracy.

The total energy (mw/cm^2) as a function of the AH-6 lamp-to-sample distance was determined with the Eppley type S pyro-heliometer. This curve is presented in Figure 12. The lamp-to-sample distance required for a specific solar intensity is computed for a given AH-6 lamp by determining the output at 25 cm. A line is drawn through this value parallel to the curve in Figure 12. Since the sun emits 13 mw/cm^2 in the ultraviolet region below 4000 A, a solar intensity of, for example, 10X requires that 130 mw/cm^2 be deposited on the specimens in question. Therefore, 340 mw/cm^2 (130 ÷ 0.38) of AH-6 radiation must be deposited to ensure 130 mw/cm^2 of ultraviolet. The lamp-to-sample distance is then obtained from Figure 12 by using the curve plotted through the output at 25 cm. For example, at 10 suns, 130 mw/cm^2 of ultraviolet and 340 mw/cm^2 of total AH-6 radiation are required; this necessitates a lamp-to-sample distance of approximately 12 cm.
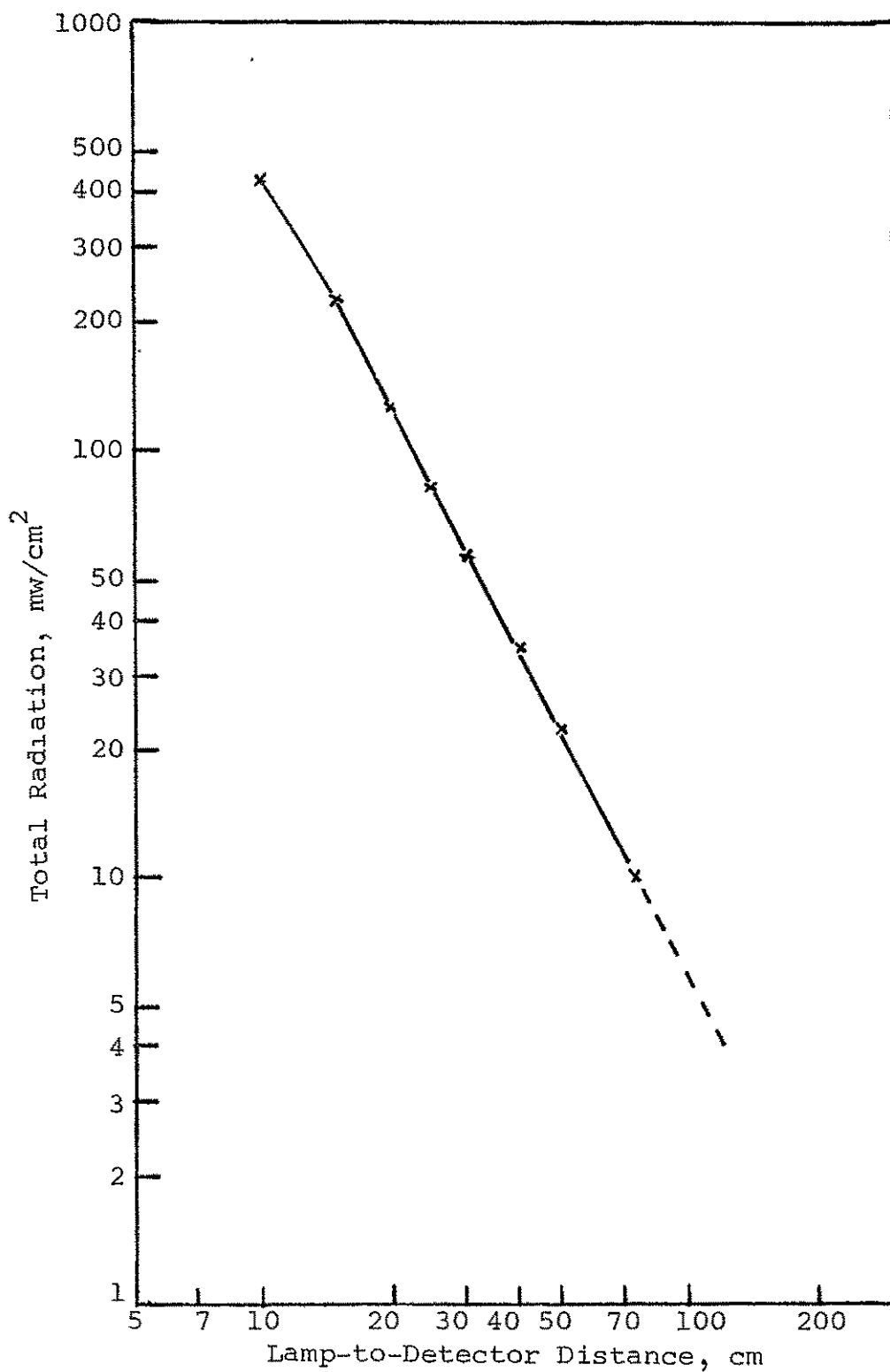
Figure 12

TOTAL AH-6 RADIATION AS A FUNCTION OF DISTANCE TO RECEIVER

APPENDIX III

CORRELATION OF INORGANIC COATING DESIGNATIONS

No. Used in This Report	No. Used in Previous Reports	No. Used in This Report	No. Used in Previous Reports
6001	1-8-2	6046	2-24-31
6002	1-9-16	6047	2-24-3
6003	1-8-F1	6048	2-24-4
6004	1-9-995	6049	2-24-6
6005	1-8-89	6050	2-24-35
6006	1-8-90	6051	2-24-36
6007	1-8-91	6052	2-24-37
6008	1-8-92	6053	2-24-7
6009	6-11-8	6054	2-24-8
6010	6-11-15	6055	2-24-9
6011	6-11-21	6056	2-24-14
6012	6-11-28	6057	2-24-28
6013	6-11-33	6058	2-24-29
6014	6-11-40	7011	1-16-77
6015	6-19-4	7012	1-16-78
6016	6-11-7	7013	1-16-79
6017	6-11-14	7015	H-24-92
6018	6-11-19	7016	1-18-85
6019	6-11-25	7019	H-24-97
6020	6-11-34	7020	1-18-86
6021	6-11-38	7021	STL 4
6022	1-9-2	7070	H-24-98
6031	2-20-16	7071	2-20-103
6032	2-20-22	7072	2-20-107
6033	2-20-26	7073	2-20-111
6034	2-20-18	7074	6-11-6
6035	2-20-19	7075	6-11-13
6036	2-20-24	7076	6-11-20
6037	2-21-13	7077	6-11-26
6038	2-21-20	7078	6-11-32
6039	2-21-27	7079	6-11-39
6041	2-24-32		
6042	2-24-33		
6043	2-24-34		
6044	2-24-25		
6045	2-24-30		

IIT RESEARCH INSTITUTE

IITRI-C6027-16

APPENDIX IV

SPECIFICATIONS FOR IITRI THERMAL-CONTROL COATINGS

Z93 Paint Specification

Materials. SP500 ZnO is obtained from New Jersey Zinc Co. The vehicle, PS7 potassium silicate, is obtained from Sylvania Electric Products Corp. The pigment is calcined at 600 to 700°C for 16 hr to obtain a mean particle size of ~0.6 μ (heating and cooling rates are not critical).

Formulation. The materials are mixed in a PBR of 4.30 and a solids content of 56.9%. A typical batch is 100 g of ZnO, 50 cc of PS7 (35% solution), and 50 cc of distilled water. The ingredients are ball-milled with porcelain balls in a dense alumina mill. The volume ratio of balls to materials is 1:3, and the total charge is <50%. A milling time of 6 hr at 70% critical speed (rpm = 54.2/$\sqrt{\text{mill radius (ft)}}$) yields a satisfactory consistency for spraying and is recommended.

The paint is prepared just before it is to be used. Shelf life for this composition is limited. Actual shelf time should not exceed 24 hr, and the mixture should be shaken occasionally to resuspend the pigment.

Application. The formulation is applied by spray-painting. The gas pressure should be clean; prepurified nitrogen is a good source. Aluminum or plastic substrates should be abraded, e.g.,

IIT RESEARCH INSTITUTE

IITRI-C6027-16

with No. 60 Aloxite metal cloth, and thoroughly washed with detergent and water.

The application technique consists of spraying at a distance of 6 to 12 in. until a reflection due to the liquid is apparent. This is followed by air-drying until the gloss is practically gone, at which time the spraying-drying cycle is repeated. A thickness of about 1 mil is acheived per cycle. Coating dimensions can therefore be predictably applied. However, hand-spraying is inherently an art and not a science, and experience must be gained by the individual painter to determine the most satisfactory technique for him.

Reapplication. The porous nature of a cured coating necessitates heavy spraying upon application of a second coat to achieve a satisfactory, finished texture. If the area to be repainted has been contaminated, it should be scrupulously cleaned with detergent and water. If desired, the paint can be removed simply by abrasion, since it is somewhat soft.

Curing. Satisfactory physical properties are obtained by an air-drying cure. Improved hardness is obtained by heat-curing at 140°C. Strict adherence to cleanliness should be observed during this step as in all the other steps. The presence of impurities can greatly decrease the stability of paints to the space environment.

Physical Properties. The coating is porous and relatively soft. It exhibits good resistance to thermal-shock treatment, which consists of immersion in liquid nitrogen followed by heating to 200°F. The departure of Z93 from the usual brittle nature of ceramics enables it to withstand stresses well. Soiling tendencies, however, are high. Cleaning can be accomplished with detergent and water. Acetone and similar organic solvents must be avoided since they leave a degradable residue.

Good protection from contamination is provided by storage under the following plastic films: Mylar, H-polymer, Lexan, Teflon Type A, and Tedlar. Samples stored under these plastics for over a year have shown no deterioration in UV-vacuum stability.

Optical Properties. Minimal solar absorptance (α) is approached at a coating thickness of 4 mils, at which the predicted α is 0.16 ± 0.01. A thickness of 5 mils yields a minimum α of 0.15. For satisfactory physical properties, coatings of 6 mils or less are desirable. The working range therefore should be between 4 and 6 mils. Emittance (ϵ) is relatively insensitive to coating thickness, and values >0.90 can be expected at 2 mils or greater.

IIT RESEARCH INSTITUTE

S-13 Paint Specification

Materials and Formulation

<div align="right">

Parts/Weight

</div>

New Jersey Zinc SP500 ZnO............................ 240
General Electric RTV-602 silicone.................. 100
General Electric SRC-05 catalyst.................. 0.6
Toluene... 184

ZnO, RTV-602, and 80 parts by weight of the toluene are
premixed and charged to a porcelain ball mill in a quantity
sufficient to fill the mill to two-thirds its volume when the
mill is from one-fourth to one-third full of grinding stones.
The paint is ground for 5 hr at approximately 70% critical speed.
The critical speed (rpm) is given by: $W_{c_s} = \sqrt{\frac{54.2}{R}}$, where R
is the radius of mill in feet. The basic charge is then
removed, and 102 parts of toluene are added to the mill in two
rinses. The mill residue and the solvent are ground in each
case until the contents are uniformly thin, but not for more
than 3 min. The contents are then added to the main charge
and the whole charge mixed thoroughly. NOTE: THE SRC-05
CATALYST IS NOT ADDED UNTIL THE PAINT IS APPLIED.

Preparation of Paint for Application. The paint is furn-
ished without the SRC-05 catalyst. The catalyst is added only
as the paint is used and to only that amount which can be applied
in about 30 min. The paint should be thoroughly stirred before
transferal to other containers or addition of catalyst. The
catalyst is added slowly with thorough mixing at 0.6% based on

IIT RESEARCH INSTITUTE

IITRI-C6027-16

resin solids (weight of RTV-602). We recommend the use of less

catalyst for optimum stability. Paint prepared at less than

0.6% (i.e., 0.4%) requires longer to cure. It will be necessary

for the user to determine the optimum catalyst concentration

for his conditions. The catalyzed paint should be allowed to

set for 5 min before it is applied to the primed surfaces.

Preparation of Surfaces for Painting. Standard surface

cleaning procedures should be used to prepare the surface for

application of the S-13 paint. In general, S-13 paint can

be applied to any surface to which the required primer can be

applied. The primer, General Electric's proprietary SS-4044,

can be applied to either anodized or zinc chromate-primed sur-

faces. It is preferable that it be applied to clean, bare

metal or to anodized surfaces, however. IT CAN NOT BE APPLIED

TO FINISHED, TOP-COATED SURFACES. SUCH SURFACES WILL REQUIRE

STRIPPING BEFORE APPLICATION OF THE SS-4044 PRIMER. Greasy

surfaces should be cleaned with standard detergent and water

before priming, and they should be thoroughly dry.

Application of Paint. The primer can be spray-applied

(Binks model 18 or comparable gun) at about 30 psi. Only about

1/2 mil of primer is required (just enough to provide a base

for the S-13 paint). The primer should be allowed to air-dry

for 1 hr before the S-13.paint is applied.

The S-13 paint can be spray-applied with a binks Model 18

spray gun (or comparable gun) at a gas pressure of about 60 psi.

Unless Missile-grade Air is available, prepurified nitrogen

IIT RESEARCH INSTITUTE

97

or prepurified air must be used. The S-13 paint should be allowed to air-cure 16 hr. IT IS IMPERATUVE THAT DUST AND DEBRIS BE KEPT OFF THE SURFACE DURING THE CURING PROCESS.

The wet film thickness of the paint can be measured by either the Pfund or the Interchemical wet-film thickness gage or other suitable gages. Dry film thickness can be measured by the Scratch thickness gage. All three gages can be obtained from the Gardner Laboratories, Inc., Bethesda 14, Maryland.

Reapplication. Soiled or damaged areas can be recoated. Soiled areas must be cleaned thoroughly with detergent and water and dried before additional S-13 paint can be applied. Damaged or gouged areas can be recoated by making a paste of S-13 in which the bulk of the solvent is omitted. Such a material can be trowelled or brushed over the damaged areas and cures tack-free within a few hours.

Physical Properties. Paint S-13 is rubbery and resilient. Therefore it can be gouged by a sharp tool with little effort. Its adherence is excellent when a primer is used, but when applied directly to a metal substrate, it can be stripped from the substrate in one piece. Because of the resiliency of the surface, dirt tends to cling to it. Dirt can be easily removed by wiping with a water-moistened CLEAN, SOFT cloth. NOTE: S-13 SHOULD NEVER BE CLEANED WITH ORGANIC SOLVENT. A 5 to 10% Alconox solution has been found to adequately clean S-13. The Alconox should be thoroughly rinsed off, however. Paint S-13 withstands more than 10 thermal-shock cycles consisting of immersion in

98

liquid nitrogen followed by rapid heating to 200°F. The paint
can be torsionally stressed to 90° without failure and withstands
repeated bending to 180°.

Optical Properties. Minimal solar absorptance is not
obtained until a thickness of nearly 10 mils is reached. The
following tabulation is provided as a guide.

Thickness (± 0.25 mils)	Solar Absorptance (± 0.01)
1	0.33
2	.27
3	.25
4	.23
5	.22
6	.21
8	.20
9	.19
10	0.18

A working range of 5 to 8 mils is recommended. For coatings
of 4 mils or thicker, the total normal emittance (200°F) is
0.90 or better.

APPENDIX V

ULTRAVIOLET-BAND-PASS FILTERS

The ultraviolet degradation of the Corning 7-54 filter used in test Q-6 is shown in Figure 13. This degradation, which caused the filter's ultraviolet transmittance to drop to only about 25% after 8 hr of irradiation, prompted the termination of Test Q-6.

Liquid filters were therefore considered. Bromine water, which selectively passes ultraviolet, was not considered because of the technical difficulties inherent in its use in a filter assembly. Highly colored transition metal salts received a great deal of attention. The absorption edge of solutions of chromium sulfate, barium chromate, barium dichromate, ceric sulfate, chromium nitrate, cobalt chloride, cobalt sulfate, cupric ammonium chloride, cupric nitrate, cupric sulfate, nickel bromide, nickel sulfate, etc. was measured. Of the many solutions examined, those of cobalt and nickel sulfate offered the most promise.

The spectra of 50% solutions of cobalt and nickel sulfate are presented in Figure 14. Neither solution was wholly ideal for our purposes. The cobalt sulfate solution permitted too much visible (red) and near-infrared radiation to pass, and the nickel sulfate solution passed 5200-A radiation.

A mixture of cobalt and nickel sulfate stabilized with sulfuric acid was found to possess optimal spectral characteristics.
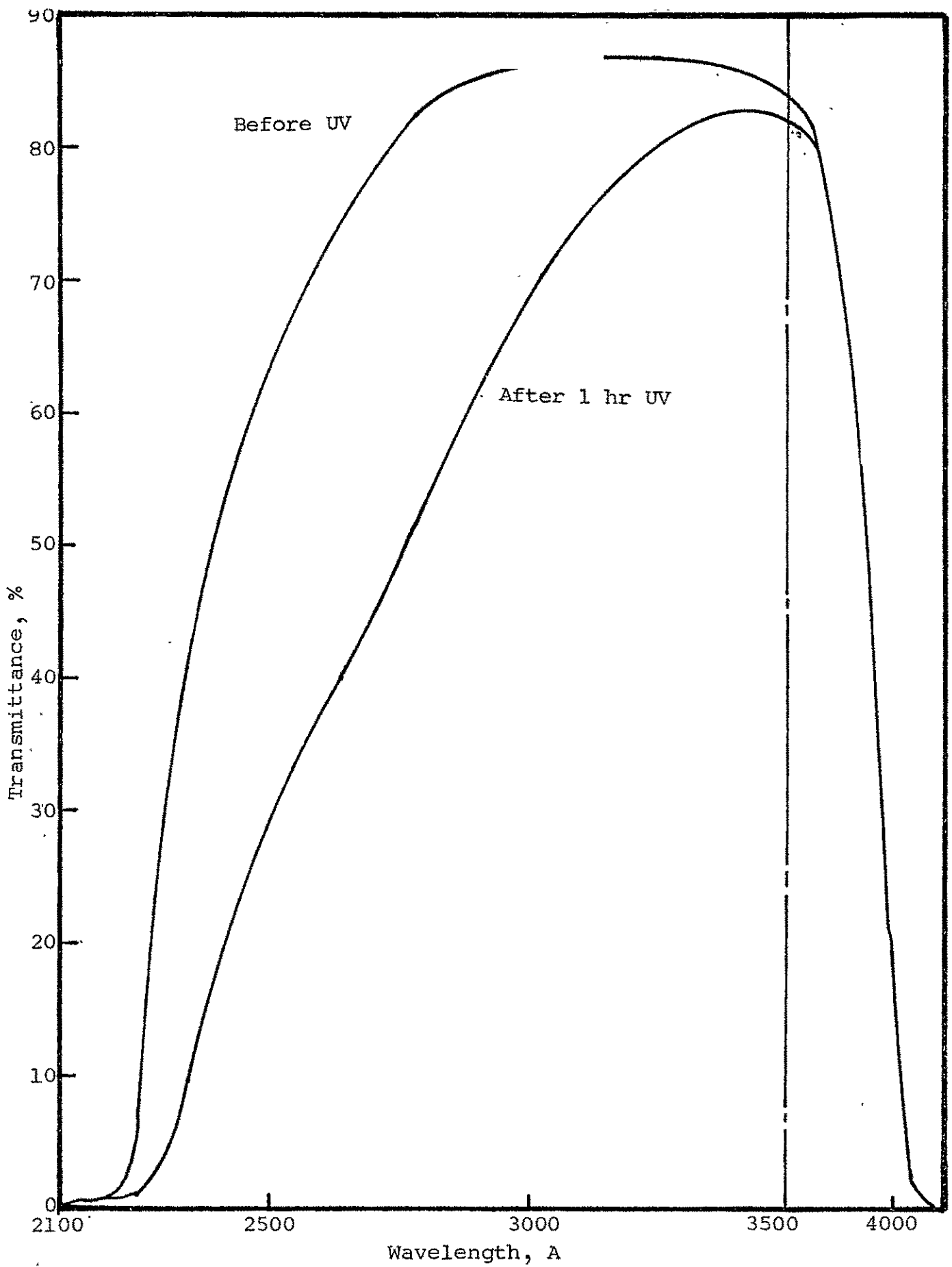
IIT RESEARCH INSTITUTE

IITRI-C6027-16

Figure 13

EFFECT OF UV ON CORNING'S 7-54 FILTER

IITRI-C6027-16
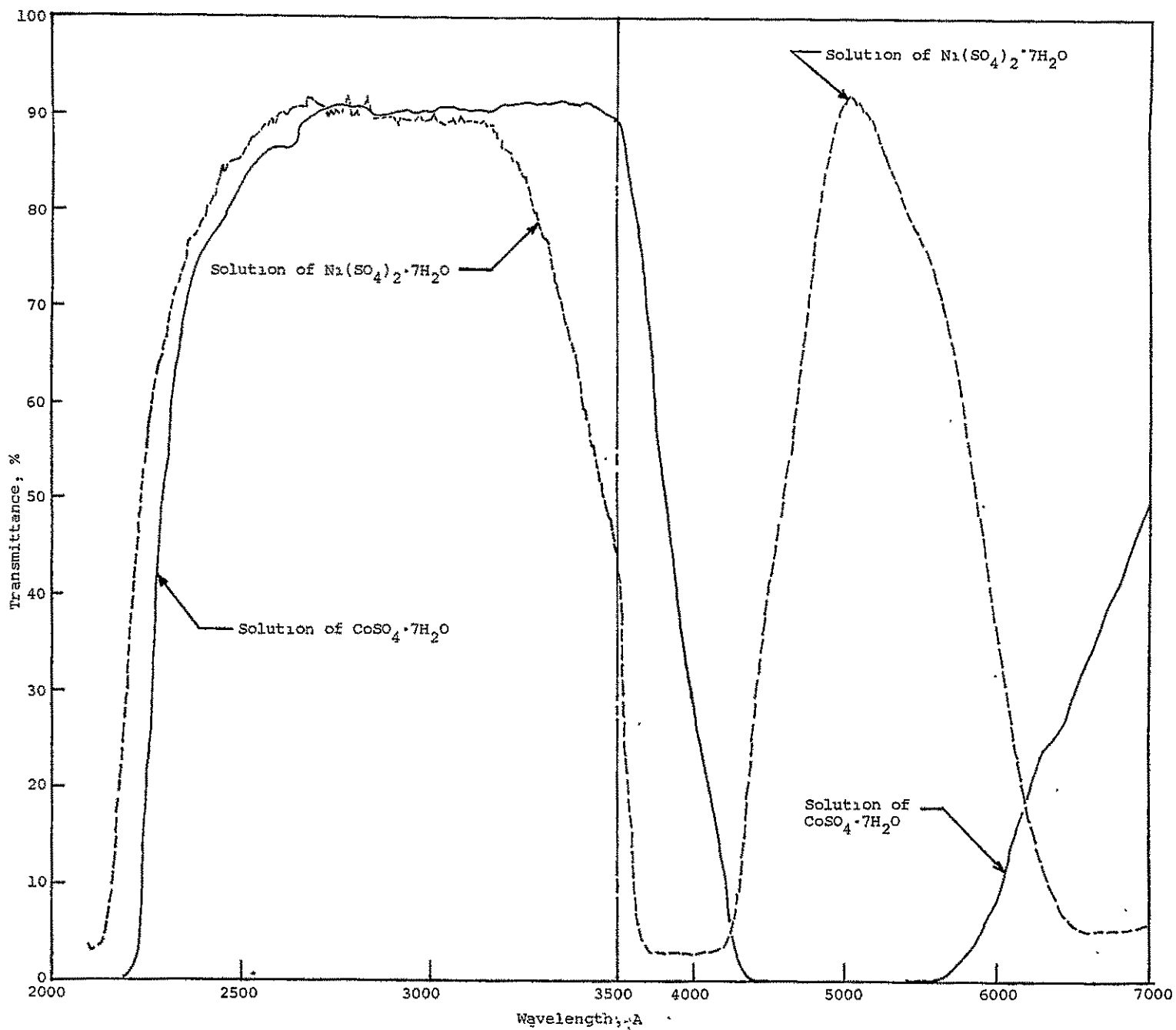
Figure 14

The formula for the solution is as follows.

Ingredient	Parts/Weight
$Ni(SO_4)_2 \cdot 7H_2O$	13.8
$CoSO_4 \cdot 7H_2O$	19.0
Conc. H_2SO_4	2.0
Water	65.2

The ultraviolet and visible transmittance spectra of the filter solution are shown in the upper curve of Figure 15. Also shown in Figure 15 is the effect of various exposures to ultraviolet. The degradation represents the effect on 1-1/2 gal of solution recirculated through the filter cell and assembly (Figures 16 and 17).

The transmittance of the cell itself after 102 hr of continuous ultraviolet irradiation is shown in the lower curve in Figure 15.
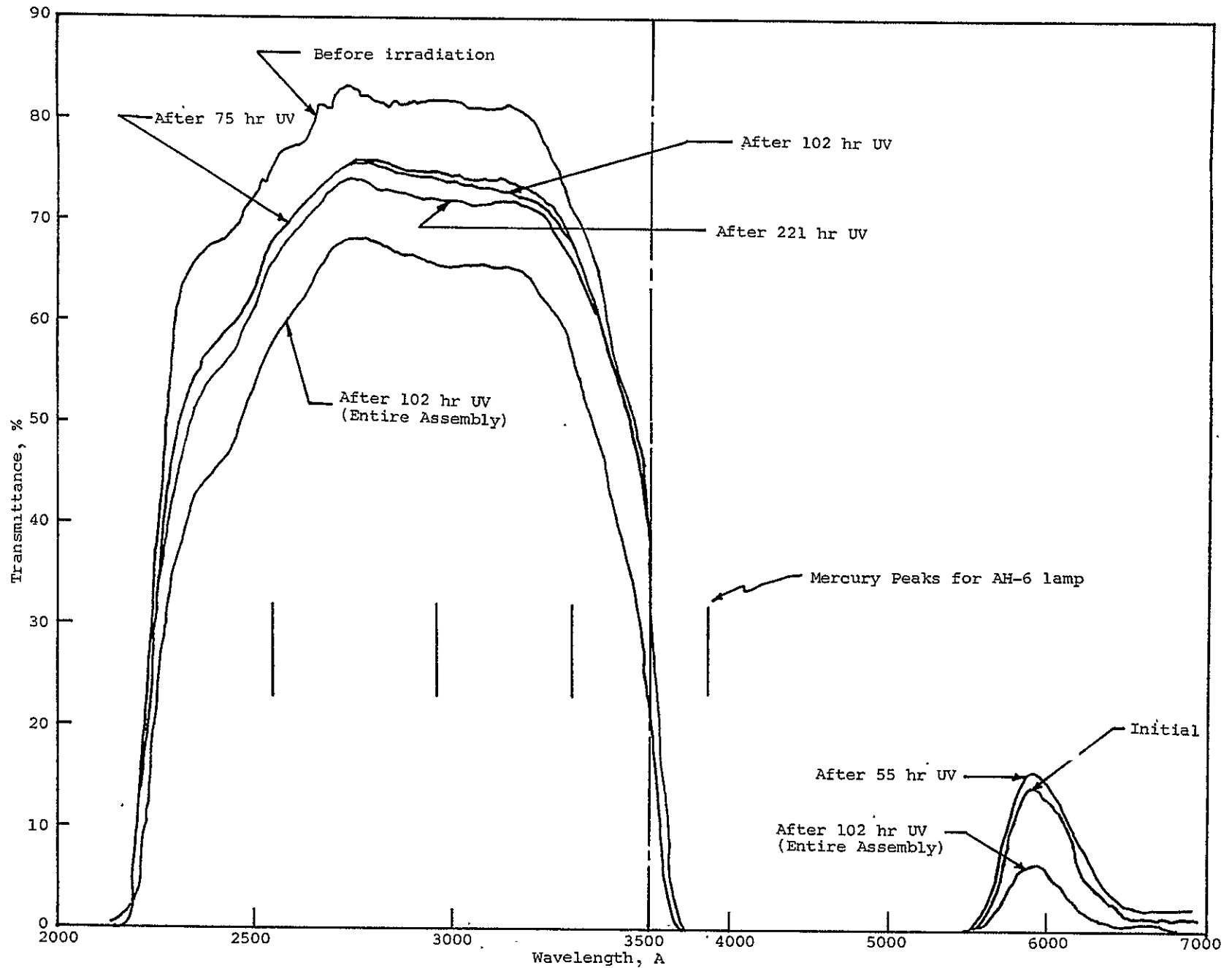
IITRI-C6027-16

Figure 15

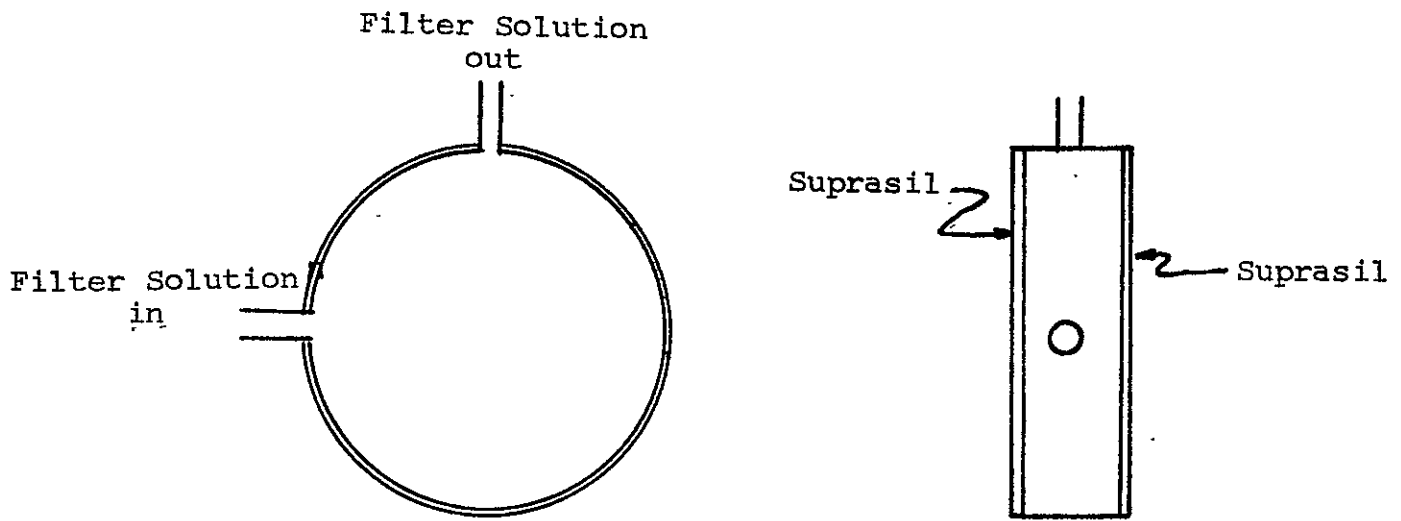EFFECT OF UV ON THE LIQUID FILTER COMPOSED OF A 50/50 MIXTURE OF COBALT AND NICKEL SULFATES
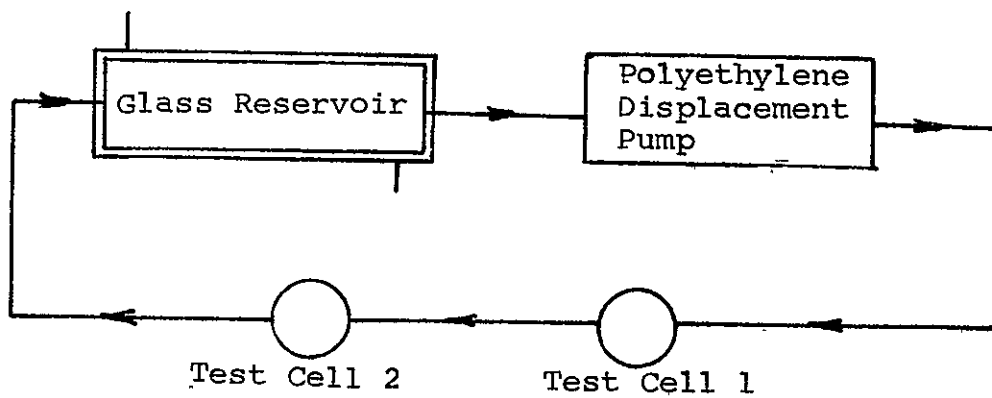
Figure 16

FILTER SOLUTION TEST CELL

Figure 17

SCHEMATIC OF LIQUID FILTER ASSEMBLY

IITRI-C6027-16

REFERENCES

1. Zerlaut, G. A. and Harada, Y., "Stable White Coatings," IIT Research Institute, Report No. IITRI-C207-25 (Summary Report), Aug. 27, 1963.

2. Zerlaut, G. A. and Harada, Y., "Stable White Coatings," IIT Research Institute, Report No. IITRI-C207-27 (Interim Report), Jan. 9, 1964.

3. Zerlaut, G. A., Harada, Y., and Berman, L. U., "Development of Space-Stable Thermal-Control Coatings," IIT Research Institute, Report No. IITRI-C6014-13 (Triannual Report), July 20, 1964.

4. Zerlaut, G. A. and Kaye, B. H., "Development of Space-Stable Thermal-Control Coatings," IIT Research Institute, Report No. IITRI-C6014-21 (Triannual Report), Feb. 23, 1965.

5. IIT Project C6025, National Aeronautics and Space Administration, Marshall Space Flight Center, Contract No. NAs-11133.

6. Zerlaut, G. A., Harada, Y., and Baldrige, J. H., "Stable White Coatings," IIT Research Institute, Report No. IITRI-C6027-7 (Semiannual Report), Aug. 13, 1964.

7. Zerlaut, G. A. and Krupnick, A. C., "An Integrating Sphere Reflectometer for the Determination of Absolute Hemispherical Spectral Reflectance," AIAA Paper 64-255, First AIAA Annual Meeting, Washington, D. C., June 29 to July 2, 1964.

8. "ZnO: Physical and Optical Properties," compiled by Linda Anderson, JPL Literature Search No. 640, Nov. 1964.

9. "Zinc Oxide Rediscovered," New Jersey Zinc Co., New York City, 1957.

10. Heiland, G., Mollwo, E., and Stöckmann, F., "Electronic Processes in Zinc Oxide," in "Solid State Physics, Advances in Research and Applications," edited by F. Seitz and D. Turnbull, Vol. 8, pp. 193-323, 1959.

11. Hutson, A. R., "Semiconducting Properties of Some Oxides and Sulfides," in "Semiconductors," edited by N. B. Hannay, Reinhold Publishing Co., pp. 541-599, 1959.

REFERENCES (cont.)

12. Zelikin, Y. M. and Zhukovskii, A.P., "The Yellow
    Luminescence of Zinc Oxide," Opt. i Spektroskopiya, 11,
    No. 3, 397-402, 1961.

13. Collins, R. J. and Thomas, D. G. "Photoconduction and
    Surface Effects with Zinc Oxide Crystals, "Phys. Rev.,
    112, No. 2, 388-395, 1958.

14. Heiland, G., "Photoconductivity of Zinc Oxide as a Surface
    Phenomenon," J. Phys. Chem. Solids, 22, 227-234, 1961.

15. Medved, D. B., "Photodesorption in Zinc Oxide Semiconductor,"
    J. Chem. Phys., 28, 870-873, 1958.

16. Melnick, D. A., "Zinc Oxide Photoconduction, An Oxygen
    Adsorption Process," J. Phys. Chem., 26, 1136-1146, 1957.

17. Barry, T. I. and Stone, F. S., "The Reactions of Oxygen
    at Dark and Irradiated Zinc Oxide Surfaces," Proc. Roy.
    Soc., A255, No. 1280, 124-144, 1960.

18. Gerritsen, H. J., Ruppel, W., and Rose, A., "Photo-properties
    of Zinc Oxide with Ohmic and Blocking Contacts," Helv. Phys.
    Acta, 30, No. 6, 504-512, 1957.

19. Thomas, D. G. and Lander, J. J., "Surface Conductivity
    Produced on Zinc Oxide by Zinc and Hydrogen," J. Phys.
    Chem. Solids, 2, 318-326, 1957.

20. Cimino, A., Molinari, E., Cramarossa, F., and Ghesini, G.,
    "The Relations between Photoconductivity and Photodesorption
    of Oxygen in Zinc Oxide," Rend. Accad. Naz. Lincei, 30,
    No. 5, 750-753, 1961.

21. Miller, P. H., "The Rôle of Chemisorption in Surface Trapping,"
    in "Photoconductivity Conference," Atlantic City, N. J.,
    Nov. 1954, edited by R. G. Breckenridge, R. B. Russell, and
    E. E. Hahn, John Wiley and Sons, Inc., New York City, 1956.

22. Mollwo, E., "Electrical and Optical Properties of ZnO," in
    "Photoconductivity Conference," Atlantic City, N.J., Nov.
    1954, edited by R. G. Breckenridge, B. R. Russell, and
    E. E. Hahn, John Wiley and Sons, Inc., New York City, 1956.

IIT RESEARCH INSTITUTE

REFERENCES (cont.)

23. Matsushita, J. S., and Nakata, T., "Infrared Absorption
    of Zinc Oxide and of Adsorbed Carbon Dioxide," J. Chem.
    Phys., <u>32</u>, 982-987, 1960.

24. Thomas, D. G., "Infrared Absorption of Zinc Oxide Crystals,"
    J. Phys. Chem. Solids, <u>10</u>, 48-51, 1959.

25. Filiminov, V. N., "Electronic Absorption Bands of ZnO and
    TiO_2 in the Infrared Region of the Spectrum," Opt. i
    Spektroskopiya, <u>5</u>, No. 6, 709-711, 1958.

26. Miloslavskii, V. K, and Kovalenko, N.A., "Absorption by
    Zinc Oxide in the Infrared Region of the Spectrum,"
    Opt. i Spektroskopiya, <u>5</u>, 614-617, 1958.

27 Collins, R. J. and Kleinman, D. A., "Infrared Reflectivity
    of Zinc Oxide," J. Phys. Chem. Solids, <u>11</u>, No. 3/4, 190-
    194, Oct. 1959.

28. McKellar, L. A., et al., "Solar Radiation Induced Damage
    to Optical Properties of ZnO-Type Pigments," Eight-Month
    Progress Report for Period June 27, 1964 to Feb. 27, 1965,
    Contract No. NAs8-11266, Report LMSC M-50-65-1, March 26, 1965.

IIT RESEARCH INSTITUTE

DISTRIBUTION LIST

This report is being distributed as follows·

Copy No.	Recipient
1-125 + repro	Jet Propulsion Laboratory California Institute of Technology 4800 Oak Grove Drive Pasadena, California Attention: Mr. Walter A. Frohn Contract Negotiator
126	Jet Propulsion Laboratory California Institute of Technology 4800 Oak Grove Drive Pasadena, California Attention: Mr. William F. Carroll Materials and Methods
127	National Aeronautics and Space Administration George C. Marshall Space Flight Center Huntsville, Alabama Attention: Mr. D. W. Gates (M-RP-T)
128	National Aeronautics and Space Administration Office of Advanced Research & Technology Washington 25, D. C. Attention: Mr. J. J. Gangler
129	National Aeronautics and Space Administration Ames Research Center Vehicle Systems Design Branch Moffett Field, California Attention· Mr. E. R. Streed
130	IIT Research Institute Division C Files
131	IIT Research Institute J. I. Bregman
132	IIT Research Institute Editors, Main Files
133	IIT Research Institute Y. Harada, Division G
134	IIT Research Institute H. L. Rechter, Division G

IIT RESEARCH INSTITUTE

IITRI-C6027-16

Copy No.	Recipient
135	IIT Research Institute W. Courtney, Division K
136	IIT Research Institute F. Iwatsuki, Division K
137	IIT Research Institute W. Jamison, Division K
138	IIT Research Institute J. Baldrige, Division C
139	IIT Research Institute J. E. Gilligan, Division C
140	IIT Research Institute S. Katz, Division C
141	IIT Research Institute E. H. Tompkins, Division C
142	IIT Research Institute D. G. Vance, Division C
143	IIT Research Institute G. A. Zerlaut, Division C
144	IIT Research Institute T. H. Meltzer, Division C

IIT RESEARCH INSTITUTE

IITRI